JACIARA LANA COSTA

ENHANCED PHOTOSYNTHETIC EFFICIENCY IN A *Solanum pennellii* CHROMOSOME 2 QTL

Dissertation presented to the Universidade Federal de Viçosa as part of requirement of the Plant Physiology Graduate Program for the obtention of the degree of *Magister Scientiae.*

VIÇOSA
MINAS GERAIS - BRAZIL
2018

Ficha catalográfica preparada pela Biblioteca Central da Universidade Federal de Viçosa - Câmpus Viçosa

T
C837e
2018

Costa, Jaciara Lana, 1992-
Enhanced photosynthetic efficiency in a *Solanum pennellii* chromosome 2 QTL / Jaciara Lana Costa. – Viçosa, MG, 2018.
ix, 41f. : il. (algumas color.) ; 29 cm.

Texto inglês.
Orientador: Adriano Nunes Nesi.
Dissertação (mestrado) - Universidade Federal de Viçosa.
Referências bibliográficas: f. 27-35.

1. *Solanum pennellii. 2.* Genética. 3. Bioquímica. 4. Variação (Genética). *5.* Metabolismo. 6. Fotossíntese. I. Universidade Federal de Viçosa. Departamento de Biologia Vegetal. Programa de Pós-Graduação em Fisiologia Vegetal. II. Título.

CDD 22. ed. 635.642

JACIARA LANA COSTA

ENHANCED PHOTOSYNTHETIC EFFICIENCY IN A *Solanum pennellii* CHROMOSOME 2 QTL

Dissertation presented to the Universidade Federal de Viçosa as part of requirement of the Plant Physiology Graduate Program for the obtention of the degree of *Magister Scientiae.*

APPROVED: July 30th, 2018

Samuel Cordeiro Vitor Martins

Paula da Fonseca Pereira

Wagner Luiz Araújo
(President)

To José Dirson e Maria dos Santos,
my dear parents, I dedicate.

"Persistence is the path to success."
Charles Chaplin

ACKNOWLEDGMENTS

To God, to be present in every moment of my life and to illuminate my path.

To my parents José Dirson e Maria dos Santos which are my examples of courage and determination. I am grateful to them for trusting and supporting me all these years. This achievement is for them.

To my brother, Dilson Lana, for the friendship and love.

To my grandparents, Geraldo e Joventina, for the love and affection.

To Robson, for the love, patience and motivation during all these years.

To all my uncles, aunts and cousins, for the affection.

To Prof. Adriano Nunes Nesi, for his advice, instruction, trust and support at all time that I needed. I am also grateful to Prof. Wagner L. Araújo for his co-supervision.

To Franklin Oliveira, for his instruction and discussions for the preparation of this work.

To Diego Costa, for all help in the construction of this work.

To my heart friends: Dani, Larissa, Amanda, Sinara, Patrícia, Gabriela, Adriana, Vivi, Samuel, Ítalo, Hellen, Regina and Alexandre. Thank you for brightening up my days.

Thanks to entire team of the Unidade de Crescimento de Plantas.

To Universidade Federal de Viçosa and Plant Physiology Program, for the opportunity to develop of this work.

Also, I would like to thank all the teachers of the Plant Physiology Program for the valuable teachings.

I am grateful to Foundation for Research Assistance of the State of Minas Gerais (FAPEMIG) for granting the scholarship.

Finally, I am sincerely grateful to all those who contributed to making this work possible.

SUMMARY

LIST OF FIGURES

LIST OF TABLES

LIST OF SYMBOLS AND ABBREVIATIONS

IL	Introgression line
A	Assimilation rate
g_s	Stomatal conductance
g_m	Mesophyll conductance
E	Transpiration
WUE_i	Intrinsic water use efficiency
WUE	Water use efficiency
R_d	Dark respiration
P_r	Photorespiration
F_v/F_m	Maximum PSII photochemical efficiency
F_v'/F_m'	Actual PSII photochemical efficiency
F_0	Minimum fluorescence
F_m	Maximum fluorescence
Fv	Variable fluorescence
ETR	Electron transport rate
NPQ	Non-photochemical quenching
PSII	Photosystem II
J_{flu},	Electron transport rate estimated by chlorophyll fluorescence parameters
C_i	Substomatal CO_2 concentration
C_c	Chloroplastic CO_2 concentration
A_{max}	Maximum photosynthetic rate
1/ϕ	Apparent quantum yield
LCP	Light compensation point
LSP	Light saturation point
J_{max}	Maximum electron transport rate
V_{cmax}	Maximum carboxylation velocity
Γ^*	Chloroplastidic CO_2 compensation point
PFD	Photon flux density
NADH	Nicotinamide adenine dinucleotide
NADPH	Nicotinamide adenine dinucleotide phosphate
ATP	Adenosine triphosphate
NaOH	Sodium hydroxide

$MgC1_2$	Magnesium chloride
DTT	Dithiothreitol
$NaHCO_3$	Sodium bicarbonate
EDTA	Etilenodiaminotetracético
EGTA	Ethylene glycol-*bis* (2-aminoethylether)- N,N,N′,N′-tetraacetic acid
GAPDH	Glyceraldehyde-3-phosphate Dehydrogenase
PGK	3-phosphoglycerate kinase
BSA	Bovine serum albumin
RuBP	Ribulose-1,5-bisphosphate
DAT	Days after transplanting
$\delta^{13}C$	Carbon isotope composition
FW	Fresh weight
DW	Dry weight
% C	Percentage of carbon
% N	Percentage of nitrogen
$[CO_2]$	Concentration of carbon dioxide
cv.	Cultivar
ANOVA	Analysis of variance

ABSTRACT

COSTA, Jaciara Lana, M.Sc., Universidade Federal de Viçosa, July, 2018. **Enhanced photosynthetic efficiency in a *Solanum pennellii* chromosome 2 QTL.** Adviser: Adriano Nunes Nesi. Co-adviser: Wagner Luiz Araújo.

Photosynthesis, one of the most important physiological processes, may be limited both by variations in diffusive and biochemical properties. Several studies have demonstrated that the genetic variation in these properties possibility to increase rates of carbon assimilation and plant yield. In a previous study utilizing a *Solanum pennellii* introgression lines (IL) population of 71 lines, the IL 2-5 and 2-6 displayed photosynthetic rates increased by up to 22% in comparison with control plants. However, understanding the genetic and physiological basis of potential mechanisms involved in the enhanced CO_2 assimilation exhibited by these lines is essential for further biotechnological applications. Thus, this study aimed to uncover the physiological factors involved in the up regulation of photosynthesis in the IL 2-5 and IL 2-6. The ILs have increased photosynthetic capacity followed by higher biomass production when compared to M82. Despite the higher photosynthetic capacity, any difference in relation to stomatal and mesophyll conductance was observed. Nevertheless, the maximum carboxylation velocity, maximum electron transport capacity and chloroplastidic CO_2 concentration correlated positively with carbon isotope composition. Further metabolite analysis also revealed that the higher photosynthetic capacity was associated with higher levels of Rubisco as well as of starch. Analysis of Western blot and data from A/C_i curve confirmed that biochemical properties are involved in genetic variation on chromosome 2 which has been related to positive effects on photosynthesis and carbon metabolism.

RESUMO

COSTA, Jaciara Lana, M.Sc., Universidade Federal de Viçosa, julho de 2018. **Caracterização de QTL relacionado à eficiência fotossintética no cromossomo 2 de *Solanum pennellii*.** Orientador: Adriano Nunes Nesi. Coorientador: Wagner Luiz Araújo.

A fotossíntese, um dos processos fisiológicos mais importantes, pode ser limitada tanto por variações nas propriedades difusivas quanto bioquímicas. Vários estudos têm demonstrado que a variação genética nestas características possibilita aumentar as taxas de assimilação de carbono e produtividade das plantas. Em um estudo anterior utilizando uma população de 71 linhas de introgressão de *Solanum pennellii* (IL), as ILs 2-5 e 2-6 apresentaram aumento nas taxas fotossintéticas em até 22% em comparação com plantas controle. Não obstante, a compreensão das bases genéticas e fisiológicas dos potenciais mecanismos envolvidos na maior assimilação de CO_2 apresentada por essas linhas é essencial para aplicações biotecnológicas futuras. Assim, este estudo teve por objetivo investigar os fatores fisiológicos envolvidos na regulação positiva da fotossíntese nas IL 2-5 e IL 2-6. As duas ILs apresentaram aumento na capacidade fotossintética seguido por maior produção de biomassa quando comparadas ao M82. Apesar da maior capacidade fotossintética, não foram observadas diferenças em relação à condutância estomática e mesofílica. No entanto, a velocidade máxima de carboxilação, a capacidade de transporte de elétrons e a concentração de CO_2 cloroplastídico correlacionaram-se positivamente com a composição isotópica de carbono. Análises metabólicas revelaram também que a maior capacidade fotossintética das ILs foi associada a elevados níveis de Rubisco, bem como de amido. A análise do Western blot e dos dados da curva A / C_i confirmou que propriedades bioquímicas estão envolvidas na variação genética no cromossomo 2 o qual tem sido relacionado a efeitos positivos na fotossíntese e metabolismo do carbono.

1. INTRODUCTION

The rapid growth population associated with global environmental changes which include scarcity of natural resources, climate changes and land degradation has threatened agricultural production (Charles, Godfray & Garnett 2014; Sundström et al., 2014). Thus, increase productivity of crop plants is essential (Tilman et al., 2002) and photosynthesis is a key process for this (Miyagawa et al., 2001; Mathan et al., 2016). However, to accomplish this aim, it is mandatory to identify genetic variation, as well as select new accessions exhibiting better photosynthetic performance under optimal and suboptimal conditions. Moreover, a better understanding of the molecular and physiological mechanisms involved in the determination of associated photosynthetic traits are clearly required for improving the photosynthetic efficiency, which could be of potential use in crop improvements from a biotechnological point of view.

It has been postulated that photosynthetic efficiency can be enhanced by improving light capture through increasing pigment contents, as well as by ameliorating light energy conversion. Furthermore, photosynthesis can be improved by reducing the resistance to CO_2 diffusion in the leaf altering the kinetic parameters of enzymes involved in carbon reduction reactions, and also by improving Rubisco biochemical capacity (Ishii et al., 2012; Weraduwage et al., 2015; Ort et al., 2015).

Global changes, particularly the rising of the atmospheric CO_2 concentration, affect significantly the carbon fixation in plants. An increment in the photosynthetic rate is observed when there is enrichment in the availability of atmospheric CO_2 for a brief period (Tomimatsu & Tang, 2016). This response arise due to the augment in the carboxylase activity of Rubisco, as well as a reduction of its oxigenase activity, leading to the diminution of the photorespiratory process, which involves the loss of carbon (Peterhansel et al., 2010). In addition, high levels of CO_2 tend to reduce stomatal conductance in leaves, leading to greater water use efficiency (Leakey et al., 2009).

In addition to environmental factors, physiological components such as diffusional and biochemical properties might also affect photosynthetic efficiency (von Caemmerer & Farquhar, 1984). Indeed, several studies have demonstrated that alterations in photosynthesis may result from diffusional limitations as those derived from changes in stomatal (g_s) and mesophyll (g_m) conductances which are dependent on leaf area and environmental factors (Flexas et al., 2007, 2012; Vrabl et al., 2009; Galmés et al., 2011). Besides diffusional, plants also display biochemical limitations related with carbon

assimilation (Sharkey, 1985; Woodrow & Berry, 1988). Intercellular CO_2 concentrations (C_i) and Rubisco activity play also important roles in the determination of CO_2 assimilation rate. It has been defined that when C_i is low, CO_2 assimilation is limited by the maximum carboxylation velocity (V_{cmax}). On the other hand, when C_i is high, CO_2 assimilation is limited by maximum electron transport rate (J_{max}) (Farquhar & Sharkey 1982).

Natural genetic variation in diffusional and biochemical traits related to photosynthesis have been verified in different plant species offering opportunity to increase the rates of carbon assimilation and yield (Geber & Dawson, 1997; Singh et al., 2014; Galmés et al., 2014). For example, Mediterranean accessions of *S. lycopersicum* cultivated under drought stress demonstrated that the genetic variation in g_m/g_s ratio would concede enhancement in transpiration efficiency in crops (Galmés et al., 2011). Furthermore, Driever et al. (2014) observed variations in the photosynthetic capacity of wheat cultivars and demonstrated that such variation could be partly explained by components related to CO_2 assimilation capacity (V_{cmax} and J_{max}). They further proposed conventional breeding for selection of cultivars with higher J_{max} contributing to Ribulose 1,5-bisphosphate (RuBP) regeneration. A good example of manipulation of RuBP regeneration capacity was demonstrated by the overexpression of the enzyme sedoheptulose-1,7-biphospatase (SBPase) in tobacco. These transgenic plants exhibited higher J_{max} values with consequent increase in photosynthetic rate and growth (Lefebvre et al., 2005).

The investigation of variation in phenotypic traits resulting from natural variation in wild species is facilitated by the use of introgression lines (ILs), which are an important genomic tool for the mapping of Quantitative trait locus (QTL) in experimental populations (Flood et al., 2011; Nunes-nesi et al., 2016). The identification of QTL demonstrates where detailed studies should be performed to identify genes and nucleotide changes responsible for a certain function (Gonzalez-Martinez et al., 2006).

The principles of ILs approach were first applied in tomato (Eshed & Zamir, 1995). The authors generated a population of ILs in which each single IL has a unique homozygous fragment of the wild tomato, *S. pennellii* (donor), introduced into the genome of the domesticated tomato, *S. lycopersicum* cv. M82 (receptor). The wild tomato, *S. pennellii*, is evolutionary rather distant specie from *S. lycopersicum* mainly differing from the second by the production of smaller fruits and in terms of physiology, metabolism and response to abiotic stresses such as drought and salinity. Despite the

differences between the two species, they are sexually compatible and can be easily crossed. In this population, 350 Restriction Fragment Length Polymorphism (RFLP) markers were used for the genotyping of lines resulting from backcrosses of ILs with *S. lycopersicum* (Eshed & Zamir, 1995). Today, due to the sequenced genome of the *S. lycopersicum* (Consortium, 2012) and *S. pennellii* (Bolger et al., 2014), it is possible to realize further genomic studies connecting phenotypic variation to differences in DNA sequence. The *S. pennellii* ILs population has been widely used to map candidate genes involved in several traits, among then carotenoid levels (Liu et al., 2003), leaf traits (Muir, Pease & Moyle, 2014), carbon isotope composition (Xu et al., 2008), enzyme activity (Steinhauser et al., 2011), drought tolerance (Gong et al., 2010), pathogen resistance (Sharlach et al., 2013), secondary metabolites (Frary et al. 2010; Alseekh et al., 2013), fruit size (Causse et al., 2004) and fruit sugar content (Baxter et al., 2005). Interestingly, a study realized with these population, based on carbon isotope composition, demonstrated that variation in stomata arrangement may improves internal CO_2 diffusion allowing greater photosynthetic efficiency in dry environments (Xu et al., 2008; Muir et al., 2014), and the most of the genetic variation in tomato g_s functioning might be explained by differences in the width and in anatomical traits of the stomatal pore (Fanourakis et al., 2015).

Recently, genomic regions involved in the regulation of fundamental physiological processes such as photosynthesis and respiration were identified in tomato (de Oliveira Silva et al., 2018). In this study a QTL for high assimilation rate (*A*) was identified in an overlapping genomic region, named as BIN 2K. This BIN is defined by two overlapping ILs, IL 2-5 and IL 2-6. The IL 2-5 exhibited up to 22% increased *A*, 50% higher nitrate content and 21% higher starch accumulation at the end of the light period in comparison with the parental line M82. Similarly, the IL 2-6 exhibited 19% increased *A*, 22% higher g_s, 42% higher levels of starch at the end of the light period and 58% higher starch turnover in comparison with M82. In agreement, the IL 2-6 also displayed higher g_s in a study about the variation in stomatal responsiveness to desiccation (Fanourakis et al., 2015). These two ILs were also evaluated for carbon isotope composition ($\delta^{13}C$), in which IL 2-5 exhibited higher values of $\delta^{13}C$ in relation to M82 and IL 2-6 (-28.1, -28.4 and -28.8, respectively) indicating the increased water use efficiency (WUE; Xu et al., 2008). The higher WUE of IL 2-5 was also verified later demonstrating that IL 2-5 is a drought-tolerant line which adapt to adverse ambient mainly through alterations in organ morphogenesis biochemical pathways (Gong et al., 2010).

In order to investigate the physiological basis for the increased photosynthetic rates previously associated with the genomic region defined as BIN 2K (de Oliveira Silva et al., 2018) a detailed physiological characterization of plants from IL 2-5, IL 2-6 and M82 was performed under ambient and high CO_2 conditions. Based on previous data (de Oliveira Silva et al., 2018), we hypothesized that the high *A* observed in these ILs results from differences in diffusive properties (stomatal or mesophyll conductance) or biochemical properties (carboxylation velocity of Rubisco and/or electron transport rate). Furthermore, given that *A* is highly affected by environmental CO_2 and Rubisco limitation is eliminated by high CO_2 concentration (von Caemmerer & Farquhar, 1981), ILs may exhibit high *A* and capacity of carbon gain under elevated CO_2.

This work provides valuable information about IL 2-5 and IL 2-6 plant physiology. These ILs displayed enhanced photosynthetic efficiency, leaf area, Rubisco and starch levels under normal conditions, as well as increased photosynthetic rates and also starch levels under high carbon dioxide concentrations. Analysis of data from A/C_i curve and from Western blot confirmed that the biochemical properties are involved in genetic variation on chromosome 2 which has been related to positive effects on photosynthesis and carbon metabolism.

2. MATERIAL AND METHODS

2.1 Plant material and experimental condition

Experiments were performed at the Unidade de Crescimento de Plantas (UCP), Universidade Federal de Viçosa (20º 45'S, 42º 15' W, 650 m altitude), Viçosa, Minas Gerais, Brazil. The seeds of the ILs, as well as the cultivar M82 were sown in trays containing the commercial substrate Tropstrato HT, Vida Verde® and allocated in a greenhouse under naturally fluctuating conditions of light intensity, temperature and relative air humidity. After germination, the seedlings were transplanted in 1.16 L pots containing the same commercial substrate, supplemented with chemical fertilizer (N:4; P_2O_5:14; K_2O: 8) in the proportion of 0.5 kg of NPK to 10.0 kg of substrate, being daily irrigated to maintain the substrate moisture close to the field capacity. The plants were kept under these conditions for four weeks until the physiological analysis and sample harvesting. The experiments comprising IL 2-5, IL 2-6 and M82 was performed in spring.

In a second experiment, the seeds from the same genotypes were germinated as described above and cultivated as described previously with the following modifications. Pots containing plants with 10 days after transplanting (DAT) were transferred to open top chambers with the following specifications, 1.6 m diameter and 1.8 m height, placed in a greenhouse under the naturally fluctuating conditions described above. The chambers were supplemented with ambient CO_2 (400 µmol CO_2 mol^{-1} air) or elevated CO_2 concentration (800 µmol CO_2 mol^{-1} air). The plants remained under these conditions for 3 weeks until further analysis.

2.2 Growth analyses

Growth parameters were determined in 4-week-old plants measuring plant height (from the base to the top of the terminal bud), stem diameter and number of leaves. Total leaf area was measured by LI-3100C Area Meter while specific leaf area was measured as described previously (Hunt et al., 2002). The dry matter accumulated in leaves, stems and roots were determined as described previously (de Oliveira Silva et al., 2018).

2.3 Measurements of gas exchange parameters and chlorophyll fluorescence

Gas exchange and chlorophyll *a* fluorescence analyses were performed simultaneously using an open-flow infrared gas exchange analyzer system equipped with an integrated fluorescence chamber (IRGA, Li-color Inc. LI-6400XT; NE). These analyses were realized during the light period, from 08:00 to 12:00 h (solar time) using the 2 cm^2 leaf chamber at 27ºC, flow rate of 300 µmol s^{-1}, 0.5 stomatal ratio (amphistomatic leaves), the leaf-to-air vapor pressure deficit range from 1.2 to 2.0 kPa and the amount of blue light was set to 10% of photon flux density (PFD) to optimize stomatal aperture. The initial fluorescence (F_0) was measured by illuminating dark-adapted leaves (1 h) with weak modulated measuring beams (0.03 µmol m^{-2} s^{-1}). A saturating white light pulse (8,000 µmol m^{-2} s^{-1}) was applied for 0.8 s to obtain the maximum fluorescence (F_m), from which the variable-to-maximum Chl fluorescence ratio was then calculated: $F_v/F_m = [(F_m - F_0) / F_m)]$. In light-adapted leaves, the steady-state fluorescence yield was measured with the application of a saturating white light pulse (8,000 µmol m^{-2} s^{-1}) to achieve the light adapted maximum fluorescence ($F_{m'}$). A far-red illumination (2 µmol m^{-2} s^{-1}) was applied after turn off the actinic light to measure

the light-adapted initial fluorescence ($F_{0'}$). The capture efficiency of excitation energy by open PSII reaction centers ($F_{v'}/F_{m'}$) was estimated following (Logan et al., 2007) and the actual PSII photochemical efficiency (φPSII) was estimated as φPSII = ($F_{m'}$– F_s)/ $F_{m'}$ (Genty et al., 1989). Dark respiration rate (R_d) was measured by the same gas exchange system after plants being at least 2 h into the dark period.

Photosynthetic light-response curves (*A*/PFD) were performed using ambient CO_2 concentration (C_a) of 400 μmol CO_2 mol^{-1} and the plants were exposed to a range of PFD in the sequence: 1000, 1500, 1300, 1100, 1000, 800, 600, 400, 300, 200, 100, 50 and 0 μmol m^{-2} s^{-1}. Variables derived from the *A*/PFD curves were estimated from adjustments of light response curve by the non-rectangular hyperbolic model (von Caemmerer, 2000). After performing photosynthetic light response curves, the light saturation point was determined and CO_2 response curves were obtained in the next day. The *A* responses to intercellular CO_2 concentration (A/C_i curves) were determined at saturating light of 1,000 μmol m^2 s^{-1} at 25º under ambient O_2 concentration (21%). Measurements were taken at ambient CO_2 concentration (C_a) of 400 μmol mol^{-1} and once the steady state was reached, the CO_2 concentrations were varied in the sequence: 300, 200, 100, 50, 400, 500, 600, 800, 1000, 1200, 1400 and 1600 μmol mol^{-1}. *A*/PFD and A/C_i curves were obtained using the second terminal leaflet of the third fully expanded leaf from the apex of 4-week-old plants.

In the second experiment, instantaneous gas exchange and chlorophyll *a* fluorescence analyses were performed as previously described, with some modifications. All measurements were performed during the light period between 8 h and 12 h (solar time) under 1,000 μmol m^{-2} s^{-1} at the leaf level (light saturation) of PFD, determined by *A*/PFD curves. The reference CO_2 concentration was set at 400 μmol CO_2 mol^{-1} air for plants at ambient CO_2 and 800 μmol CO_2 mol^{-1} air for plants under elevated CO_2 concentration. Instantaneous measurements were obtained using the second terminal leaflet of the third fully expanded leaf from the apex of 4-week-old plants. R_d was determined by the same gas exchange system as described previously.

2.4 Estimation of mesophyll conductance (g_m), maximum rate of carboxylation (V_{cmax}), maximum rate of carboxylation limited by electron transport (J_{max}), and photosynthetic limitations

The concentration of CO_2 in the carboxylation sites (C_c) was calculated following Harley et al. (1992) where the conservative values of Γ^* for tomato was taken from (Hermida-Carrera et al., 2016). Then, g_m was estimated as the slope of the A vs C_i-C_c relationship as $g_m = A/(C_i - C_c)$. Thus, estimated g_m is an averaged value over the points used in the relationship (C_i < 300 µmol mol^{-1}). g_m was estimated by the Ethier & Livingston (2004) method, which fits A/C_i curves with a nonrectangular hyperbola version Farquhar-von Caemmerer-Berry model, based on the hypothesis that g_m reduces the curvature of the Rubisco-limited portion of an A/C_i curve.

The parameters from A/C_i and A/C_c, as maximum carboxylation velocity (V_{cmax}) and maximum capacity for electron transport rate (J_{max}) were calculated by fitting the mechanistic model of CO_2 assimilation (Farquhar et al., 1980), using the C_i and C_c based on temperature of kinetic parameters of Rubisco (K_c and K_o). V_{cmax}, J_{max}, and g_m were normalized to 25°C using the temperature response and plug-in equations described by Sharkey et al. (2007).

The photosynthetic limitations were estimated based on the approach described by (Grassi & Magnani, 2005). From combined measurements of fluorescence and gas exchange, we estimated the photorespiration rate (P_r) according to (Valentini et al., 1995).

2.5 Carbon isotope composition, Carbon content and Nitrogen content

The second terminal leaflet of the third fully expanded leaf was harvested in the middle of the light period (12:00 h, solar time) from the apex of 4-week-old plants. The samples were oven-dried 72ºC for 24h and ground to a fine powder. The carbon content and carbon isotope composition were determined using an isotopic ratio mass spectrometer (ANCA-GLS Sercom, Crewe, UK). The carbon isotope composition was analyzed as described by (DaMatta et al., 2002). The total nitrogen content was determined using the Kjeldahl digestion technique (Bremner & Mulvaney, 1965).

2.6 Metabolite analyses

Samples from fully expanded leaves were harvested in five different time points (beginning, middle and end of the light period, as well as middle and end of the dark period) from 4-week-old plants. The material was frozen in liquid nitrogen and stored at -80°C for further analyses. Samples were homogenized and aliquots of approximately 20

mg were subjected to hot ethanol extraction as described by (Cross et al., 2006). The levels of starch, glucose, fructose and sucrose were measured as described (Fernie et al., 2001). The levels of chlorophyll (*a* and *b*) and nitrate contents were determined as detailed by (Sulpice et al., 2009) and malate and fumarate as Nunes-nesi et al. (2007). Total protein and total amino acids contents were determined as reported by Cross et al. (2006).

2.7 Evaluation of Rubisco activity

For Rubisco, 50 mg of leaf material collected in the middle of the light period was used. The protein extraction was performed exactly as previously described by Gibon et al. (2004). The Rubisco activity was determined spectrophotometrically by following the oxidation of NADH at 340 nm. The basal Rubisco activity was determined as previously described (Sulpice et al., 2007), with minor modifications. Briefly, 20 µl of diluted extract was incubated in a reaction buffer consisting of Bicine 100 mM pH 8,0 in NaOH; EDTA 1 mM pH 8; $MgC1_2$ 15 mM (for basal activity) e 20 mM (for total activity); DTT 10 mM; $NaHCO_3$ 5 mM (for basal activity) and 10 mM (for total activity); NADH 0,5 mM; ATP 2 mM; phosphocreatine kinase (2 units mL^{-1}); GAPDH (40 units mL^{-1}); 3-phosphoglycerate kinase - PGK (10 units mL^{-1}); phosphocreatine 5 mM; BSA 0,1%. The reaction was started by the addition of ribulose-1,5-bisphosphate (RuBP) to a final concentration of 20 mM. The total Rubisco activity was measured after 25 min of incubation at 25 °C.

2.8 Protein extraction and Western blot analysis

Total soluble protein was extracted from 200 mg (fresh weight) of leaf tissue according to the protocol of Vasconcelos et al. (2005). Protein was quantified by using the Bradford quantification method (Bradford, 1976). A quantity of 40 µg of total protein was subjected to a solution containing sample buffer (125 mM Tris-HCl, pH 6.8, containing SDS 4%, 20% glycerol, 4% 2-mercaptoethanol and 0.1% bromophenol blue). The samples were separated using 12% glycine sodium dodecyl sulfate polyacrylamide gel electrophoresis (Glycine–SDS-PAGE). The marker used was Amersham ECL High-Range Rainbow (GE Healthcare). The proteins were electrophoretically transferred to nitrocellulose membrane (0.45 µm; Bio-Rad) by the method of Towbin et al. (1979). The membranes were blocked for 2h with 3% (w/v) Bovine serum albumin in Tris-buffered

saline (2 M Tris-HCl, pH 7.4, containing 5 M NaCl and 10% tween). The blots were then incubated for 2h with specific antibodies raised in rabbit (serum diluted 1:12000 large subunit - AS03 037 code). The membranes were treated for 2h with bridging antibodies (Anti-rabbit HRP-conjugated secondary antibodies GE Healthcare, RPN2108 code) diluted 1:10000. Rubisco subunits were visualized with substrate solution (10 mg of 3,3' -Diaminobenzidine mixed with 10 mL of Tris-buffered saline and 10 µL of H_2O_2). All steps were performed at room temperature. Tween-20 in Tris-buffered saline was used for washing (five times for 5 min between all treatments mentioned above) as well as for the dilution of antibodies. The bands on immunoblots were quantified by densitometry using the ImageJ program (Schneider et al., 2012). Data were normalized by standard marker (~50 kDa) and are expressed in fold change.

3. EXPERIMENTAL DESIGN AND STATISTICAL ANALYSES

The experiments were performed in a randomized complete block design. The data were submitted to analysis of variance (ANOVA), for the second experiment two factors were considered corresponding to two environments: ambient and elevated CO_2 concentration. In order to verify the statistical difference between the genotypes, the means were compared using a most rigorous test in comparative statistics, the Tukey test ($P < 0.05$) using the GENES program (Cruz, 2013).

4. RESULTS

4.1 Growth phenotypes of plants from ILs with altered photosynthetic rates

ILs with increased *A* were selected based on previously published data from two years experiment (de Oliveira Silva et al., 2018). When plants from this two ILs were grew in the greenhouse side by side with M82 control, a clear increase in the growth of the aerial parts of the ILs was observed (Figure 1). Detailed examination revealed that the ILs increased total leaf area and specific leaf area (only for IL 2-5) in comparison to the M82 plants (Figure 1A and 1B). The ILs exhibited also an increase in biomass accumulation in the branches and roots (Figure 1D and 1E). On the other hand, leaf (Figure 1C), shoot (Figure 1F) and total dry weight (Figure 1H) were significantly only for IL 2-6. Despite the significant increase in total leaf area observed for the two ILs

(Figure 1A), no alterations in biomass allocation as indicated by similar root:shoot ratios were observed (Figure 1G).

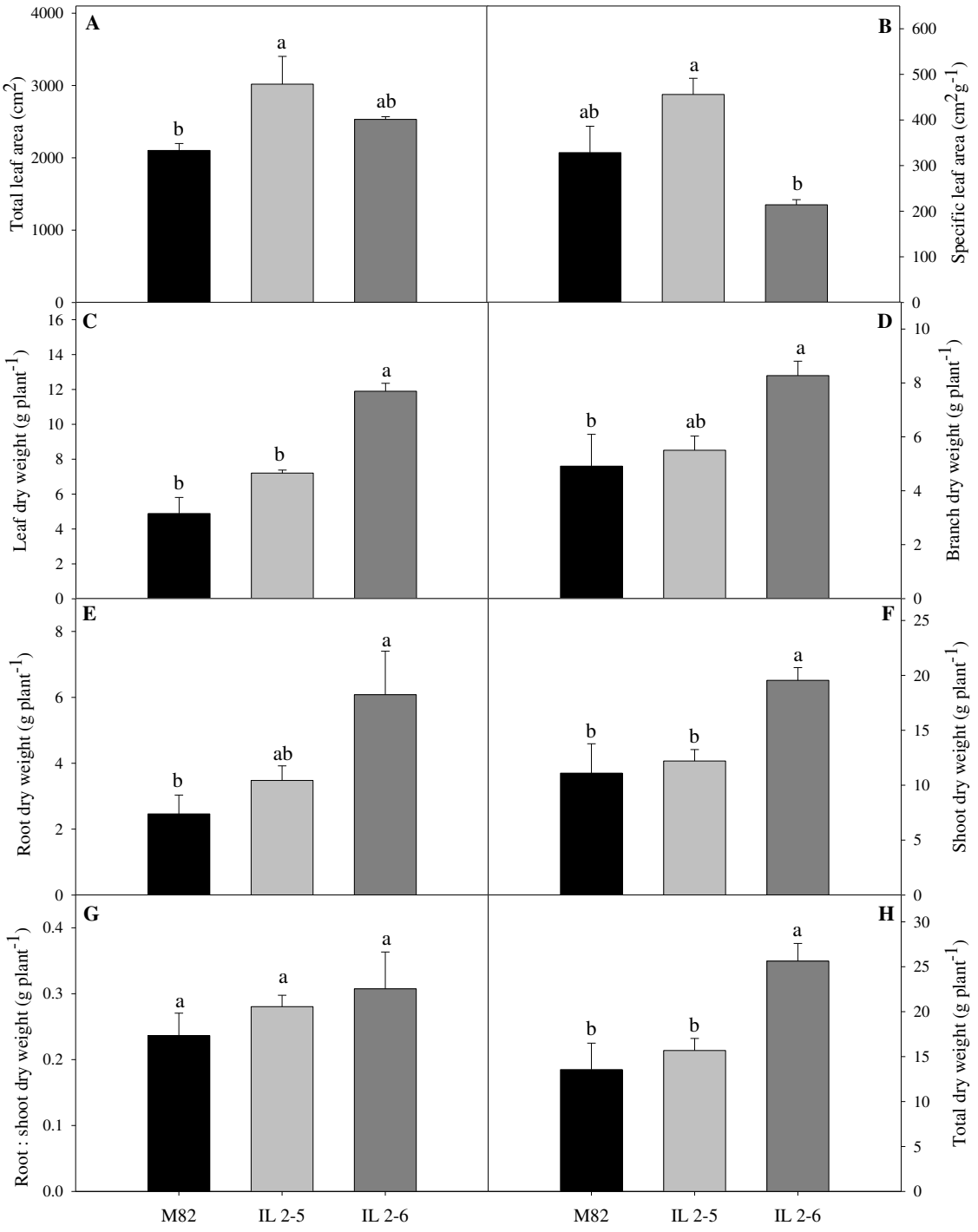

Figure 1. Growth phenotypes of 4-week-old plants from two ILs of *Solanum pennellii* into a genetic background of *Solanum lycopersicum* (M82).

Total leaf area **(A)**; Specific leaf area **(B)**; Leaf dry weight **(C)**; Branch dry weight **(D)**; Root dry weight **(E)**; Shoot dry weight **(F)**; Root : shoot dry weight ratio **(G)**; Total dry weight **(H)**. Values are presented as means ± *SE* (n = 6). Means that differ significantly between ($P < 0.05$) by the Tukey test are accompanied by different letters.

4.2 Gas exchange and chlorophyll *a* fluorescence parameters of ILs with altered photosynthetic rates

Since two ILs displayed higher photosynthetic rate in our previous study (de Oliveira Silva et al., 2018) and displayed altered plant growth, we next decided to investigate the photosynthetic capacity of these ILs by varying light intensities and CO_2 concentrations. To this end, we performed *A*/PFD and A/C_i curves. Surprisingly, despite the higher biomass accumulation in the ILs, they did not exhibit higher CO_2 assimilation rates in different light intensities (Figure 2A). However, the apparent quantum yield ($1/\phi$) was significantly higher in the ILs (Supplementary table 1). Further analysis indicated that the ILs displayed similar stomatal conductance (g_s) and fluorescence related parameters under normal CO_2 condition (Table 1). The exception was a significant increase in electron transport rate (J_{flu}), estimated by chlorophyll fluorescence parameters in the ILs (Table 1). Based on that, we next decided to further characterize photosynthesis in these lines under variable CO_2 concentrations by using A/C_i and A/C_c analysis. Interestingly, an increase in photosynthetic rates was observed in A/C_i and A/C_c curves in ILs (Figure 2B and 2C). From A/C_i curve, photosynthesis was ~14% higher in the ILs under CO_2 saturating conditions (800 µmol CO_2 m^{-2} s^{-1}, specifically; Figure 2B). On the other hand, from A/C_c curve, assimilation rate was ~11% higher in the ILs under normal CO_2 conditions (Figure 2C). The ILs exhibited lower values of chloroplastic CO_2 concentration (C_c), probably due to the higher values of maximum carboxylation velocity based on C_c ($V_{cmax}\_C_c$) (Table 2). In addition, the maximum capacity for electron transport rate (J_{max}) was significantly higher in the ILs in comparison to M82, when expressed in C_c bases (Table 2). By estimating the additional parameters derived from the A/C_i response curves, it was verified that the two ILs do not have altered mesophyll conductance (g_m) neither stomatal and other mesophyll limitations (Table 2). Nevertheless, it is important to note the similar values of $J_{max}\_ C_i$: $V_{cmax}\_ C_i$ and $J_{max}\_C_c$: $V_{cmax}\_ C_c$ ratios among the genotypes. In addition, V_{cmax} and J_{max} in C_c base were superior to the values in C_i basis, independent of the analyzed genotype (Table 2). Altogether, these data corroborate our proposal that the ILs have an important role for photosynthetic performance in tomato.

Regarding carbon isotope composition ($\delta^{13}C$), the leaves presented an average of $\delta^{13}C$ around -29.00 ‰ which correspond to the values reported in the literature, for species with C3 photosynthetic cycle ranging from -20.0 ‰ to -32.0 ‰ (Farquhar et al.,

1989). As previously found by Xu et al., (2008), only the IL 2-5 exhibited significant less negative values of $\delta^{13}C$ in relation to M82 plants (Figure 2D).

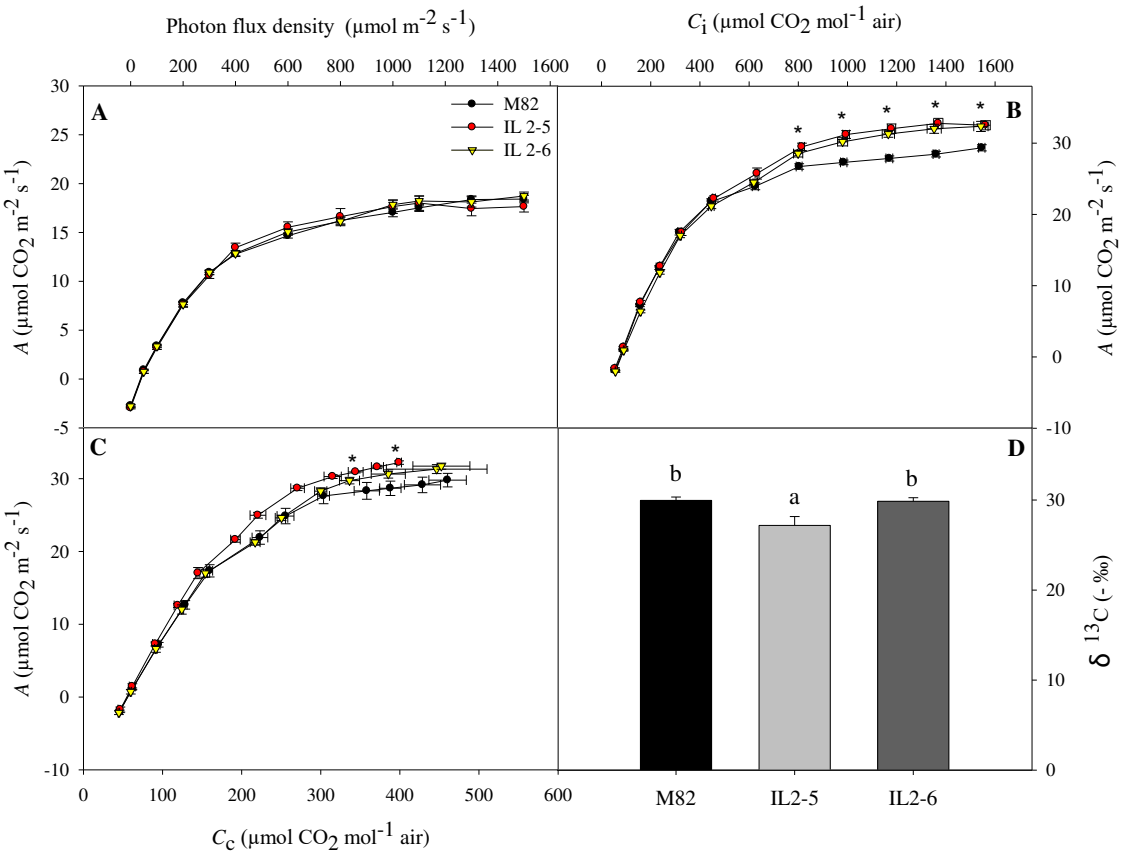

Figure 2. Curves of assimilation rate and carbon isotope composition of 4-week-old plants from two ILs of *Solanum pennellii* into a genetic background of *Solanum lycopersicum* (M82).

Assimilation rate (*A*) as a function of photon flux density intensities (PFD) **(A)**; Assimilation rate (*A*) as function to substomatal CO_2 concentrations (C_i) **(B)**; Assimilation rate (*A*) as function to chloroplastic CO_2 concentrations (C_c) **(C);** Carbon isotope composition ($\delta^{13}C$) **(D)**. Values are presented as means ± *SE* (n = 6). Means that differ significantly between ($P < 0.05$) by the Tukey test are accompanied by different letters. Asterisks indicate significant differences of the ILs in relation to M82 ($P < 0.05$) according to the Tukey test.

Table 1. Gas exchange and chlorophyll *a* fluorescence parameters of 4-week-old plants from two ILs of *Solanum pennellii* into a genetic background of *Solanum lycopersicum* (M82). Values are presented as means ± *SE* (n = 6). Means that differ significantly between ($P < 0.05$) by the Tukey test are accompanied by different letters.

Parameters*	**M82**	**IL 2-5**	**IL 2-6**
A (µmol CO_2 m^{-2} s^{-1})	17.34 ± 1.12 **a**	17.34 ± 1.04 **a**	17.00 ± 1.11 **a**
g_s (mol H_2O m^{-2} s^{-1})	0.42 ± 0.03 **a**	0.40 ± 0.03 **a**	0.43 ± 0.04 **a**
E (mmol H_2O m^{-2} s^{-1})	5.10 ± 0.40 **a**	4.64 ± 0.37 **a**	5.00 ± 0.42 **a**
WUE_i (A / g_s)	39.18 ± 3.74 **a**	43.61 ± 2.44 **a**	40.65 ± 2.89 **a**
WUE (A / E)	3.62 ± 0.27 **a**	3.96 ± 0.27 **a**	3.59 ± 0.24 **a**
R_d (µmol CO_2 m^{-2} s^{-1})	2.04 ± 0.63 **a**	2.24 ± 0.55 **a**	2.36 ± 0.55 **a**
P_r (µmol CO_2 m^{-2} s^{-1})	7.62 ± 0.37 **a**	8.28 ± 0.31 **a**	8.18 ± 0.36 **a**
F_v / F_m	0.800 ± 0.002 **a**	0.797 ± 0.003 **a**	0.794 ± 0.003 **a**
F_v' / F_m'	0.62 ± 0.001 **a**	0.61 ± 0.002 **a**	0.61 ± 0.011 **a**
J_{flu} (µmol m^{-2} s^{-1})	145.79 ± 8.16 **b**	166.64 ± 7.27 **a**	163.38 ± 7.90 **ab**

* A, Assimilation rate; g_s, stomatal conductance; E, transpiration rate, WUE_i, sub-stomatal CO_2 concentration; C_c : Chloroplastic CO_2 concentration; g_m, mesophyll conductance to CO_2 estimated according to the Harley and Ethier; $V_{cmax}\_C_i$ or C_c, maximum carboxylation capacity based or C_i or C_c ; $J_{max}\_C_i$ or C_c: maximum capacity for electron transport rate based on C_i or C_c.

Table 2. Photosynthetic characterization of 4-week-old plants from two ILs of *Solanum pennellii* into a genetic background of *Solanum lycopersicum* (M82). Values are presented as means ± *SE* (n = 6). Means that differ significantly between ($P < 0.05$) by the Tukey test are accompanied by different letters.

Parameters*	**M82**	**IL 2-5**	**IL 2-6**
C_i (µmol CO_2 mol^{-1})	313.02 ± 4.29 **a**	303.88 ± 4.77 **a**	312.65 ± 3.45 **a**
C_c (µmol CO_2 mol^{-1})	164.41 ± 4.55 **a**	148.15 ± 5.80 **b**	150.20 ± 6.55 **ab**
g_m_Harley (mol CO_2 m^{-2} s^{-1} bar)	0.181 ± 0.007 **a**	0.187 ± 0.027 **a**	0.196 ± 0.027 **a**
g_m_Ethier (mol CO_2 m^{-2} s^{-1} bar)	0.205 ± 0.019 **a**	0.211 ± 0.027 **a**	0.219 ± 0.017 **a**
V_{cmax}_C_i (µmol CO_2 mol^{-1})	47.80 ± 3.26 **a**	54.06 ± 4.59 **a**	51.37 ± 3.87 **a**
V_{cmax}_C_c (µmol CO_2 mol^{-1})	89.30 ± 6.34 **b**	115 ± 10.40 **a**	102.37 ± 5.50 **ab**
J_{max}_C_i (µmol CO_2 mol^{-1})	113.86 ± 7.43 **a**	124.54 ± 6.40 **a**	120.32 ± 6.10 **a**
J_{max}_C_c (µmol CO_2 mol^{-1})	140.82 ± 7.14 **b**	164.53 ± 7.67 **a**	157.82 ± 4.85 **a**
J_{max}_C_i : V_{cmax}_C_i	2.32 ± 0.08 **a**	2.44 ± 0.12 **a**	2.55 ± 0.13 **a**
J_{max}_C_c : V_{cmax}_C_c	1.54 ± 0.07 **a**	1.52 ± 0.08 **a**	1.63 ± 0.06 **a**
Stomatal limitation	0.190 ± 0.015 **a**	0.222 ± 0.013 **a**	0.194 ± 0.018 **a**
Mesophyll limitation	0.326 ± 0.020 **a**	0.340 ± 0.027 **a**	0.331 ± 0.021 **a**
Biochemical limitation	0.476 ± 0.018 **a**	0.425 ± 0.013 **a**	0.462 ± 0.016 **a**

*C_i, Substomatal CO_2 concentration; C_c, chloroplastic CO_2 concentration; g_m, mesophyll conductance to CO_2 estimated according to the Harley and Ethier method; V_{cmax}_C_i or C_c, maximum carboxylation velocity based on C_i or C_c; J_{max}_C_i or C_c, maximum capacity for electron transport rate based on C_i or C_c.

4.3 Rubisco activity in leaves from ILs with altered photosynthetic rates

Whereas the ILs displayed increase in V_{cmax}, we further measured Rubisco activity. Surprisingly, the measurement of Rubisco activity immediately upon extraction, which reflects activity *in vivo*, was clearly unaltered in plants from both ILs in comparison with M82 plants (Supplementary figure 3A-C). Despite that, a minor increase in the carboxylation potential, which was determined by incubating the extracts with high concentrations of CO_2 and Mg^{2+} prior to assay, was observed in plants from IL 2-5 (Supplementary figure 3C). Taken together, these results indicated a slight increase in the activation state of Rubisco only in plants from the IL 2-5 (Supplementary figure 3C).

4.4 Photosynthetic carbon and nitrogen metabolism in illuminated leaves of plants from ILs with altered photosynthetic rates

We next analyzed the carbohydrate content in leaves from 4-week-old plants during diurnal cycle. This analysis revealed increased starch contents in leaves at the end of the light period in the ILs in relation to M82; on the other hand, at the end of dark period and at the beginning of the light period the starch levels in the ILs decreased, which may indicate greater night starch degradation (Figure 3A). We further analyzed other abundant metabolites in illuminated tomato leaves (Figure 3 B-D). The levels of glucose were increased at the end of the light period and sucrose in the middle of the night in the IL 2-5 (Figure 3B and 3D), whereas no significant increase was observed in the levels of fructose (Figure 3C). The two ILs were also characterized by unaltered malate and fumarate contents, except for a reduction in malate levels at the beginning of the day (Figure 3E-F) and in fumarate at the end of the night. In spite of the higher levels of the main carbohydrates in the leaves of the ILs in comparison to M82, the percentage of carbon in leaves was around 40% in all analyzed genotypes (Supplementary figure 3D). The total chlorophyll content were unaltered in the ILs (Figure 4A), while the chlorophyll *a/b* ratio exhibited an increase in the IL 2-6 compared to IL 2-5 (Figure 4B). In contrast, proteins levels increased by up to 21% in the IL 2-5 and 18% in the IL 2-6 in comparison to M82 (Figure 4C). Nothwhorthing, total amino acids and nitrate levels as well as percentage of nitrogen did not differ between the genotypes (Figure 4D, 4E and 4F).

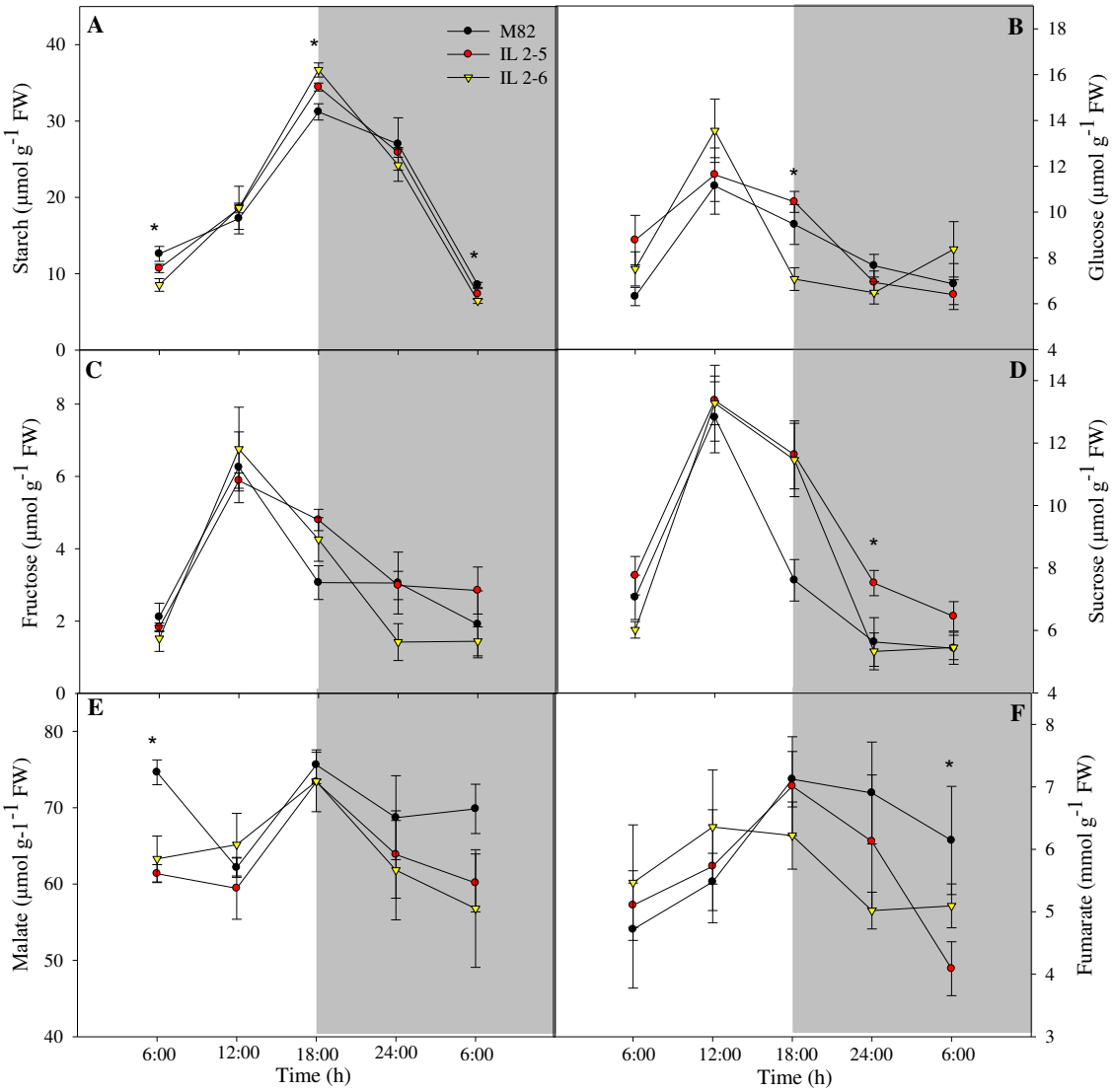

Figure 3. Changes in the metabolite contents involved in carbon metabolism of 4-week-old plants from two ILs of *Solanum pennellii* into a genetic background of *Solanum lycopersicum* (M82).

Starch **(A)**; Glucose **(B)**; Fructose **(C)**; Sucrose **(D)**; Malate **(E)**; Fumarate **(F)**. Values are presented as means ± *SE* (n = 6). Asterisks indicate significant differences of the ILs in relation to M82 ($P < 0.05$) according to the Tukey test. FW: Fresh weight.

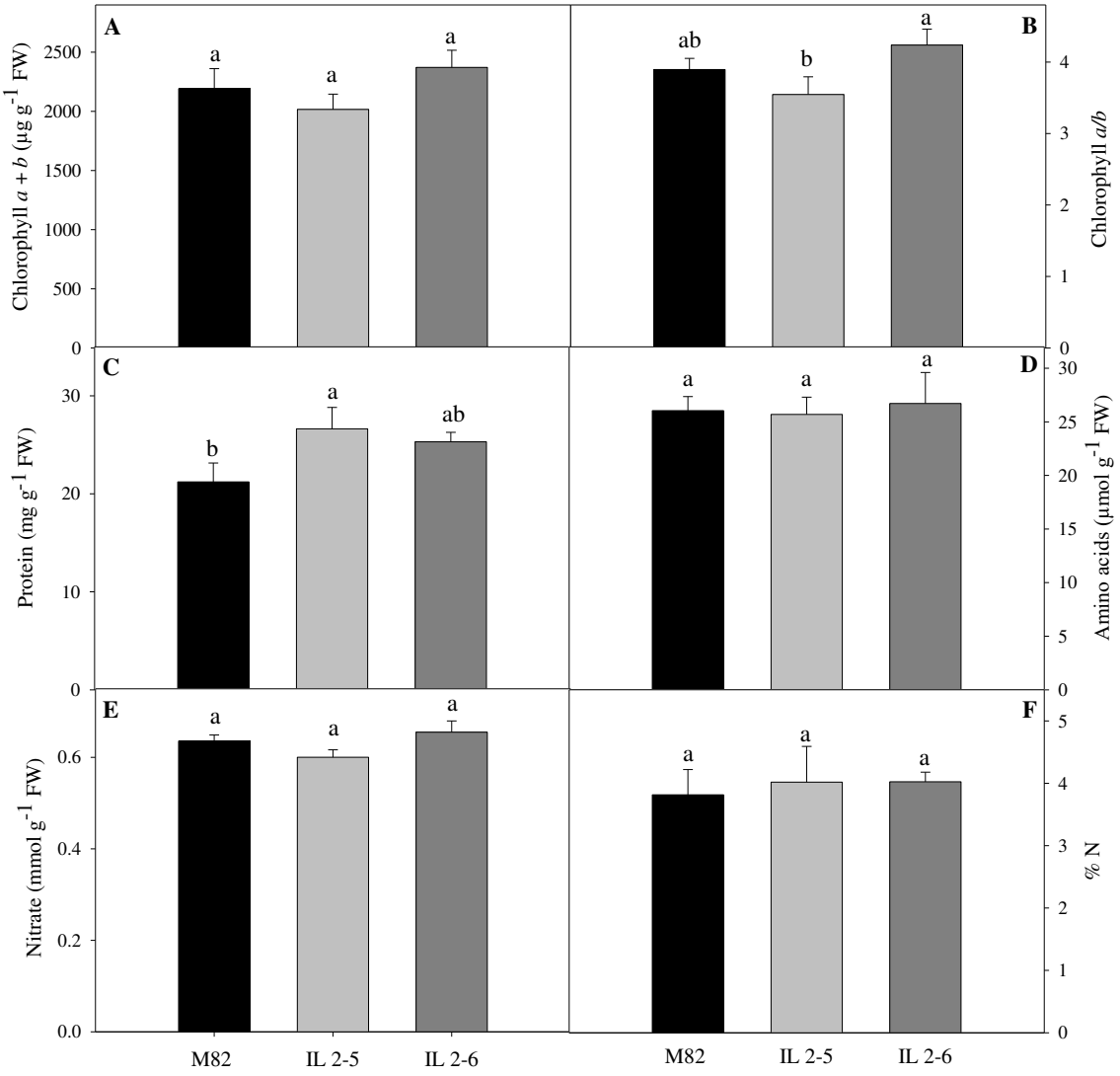

Figure 4. Changes in the metabolite contents involved in nitrogen metabolism, as well as percentage of nitrogen of 4-week-old plants from two ILs of *Solanum pennellii* into a genetic background of *Solanum lycopersicum* (M82).

Chlorophyll *a* + *b* **(A)**; Chlorophyll *a/b* ratio **(B)**; Protein **(C)**; Amino acids **(D)**; Nitrate **(E)**; Nitrogen percentage **(F)**. Values are presented as means ± *SE* (n = 6). Means that differ significantly between ($P < 0.05$) by the Tukey test are accompanied by different letters. FW: Fresh weight.

4.5 Rubisco content is increased in leaves of plants from ILs with altered photosynthetic rates

Rubisco is an essential enzyme in the photosynthetic process and its amount is strictly associated to the photosynthetic capacity (Palmqvist et al., 1998). Since the ILs displayed increase in protein content, we next decided to analyze the Rubisco levels by Western blot with antibodies against its large subunit (RbcL). The results evidenced an enhancement of approximately 20% of RbcL in levels of the ILs compared to M82 (Figure 5B).

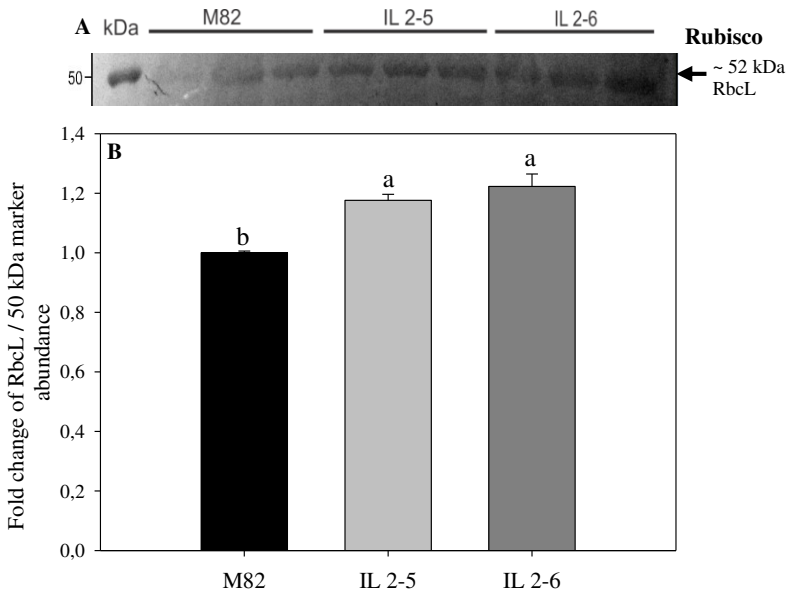

Figure 5 Rubisco large subunit (RbcL) is increased in 4-week-old plants from two ILs of *Solanum pennellii* into a genetic background of *Solanum lycopersicum* (M82).
The levels of RbcL were determined by Western blot **(A)**; Quantification of western-blot results **(B)**. Signal intensities were measured using ImageJ software and normalized to the amount of loaded marker (~50 kDa). Values are expressed as fold change over the control M82 and presented as means ± *SE* (n = 3). Means that differ significantly between ($P < 0.05$) by the Tukey test are accompanied by different letters.

4.6 Elevated CO_2 concentration modifies the photosynthetic parameters, as well as metabolites from carbon and nitrogen metabolism in leaves from ILs with altered photosynthetic rates

Given the fact that our previous results suggested that the ILs have increased photosynthetic capacity, indicated by the higher assimilation rate at saturating external CO_2 concentration, as well as increased electron transport rate (J_{flu}), we comparatively analyzed M82 plants and the two ILs growing for 3 weeks under ambient and elevated CO_2 concentration. Under ambient CO_2 conditions, no differences between ILs and M82 were observed in A (Figure 6A), g_s (Figure 6B) and R_d (Figure 6F). As observed in the previous experiment, the ILs displayed a significant increase of ETR (Figure 6D).

In agreement with our previous results, under elevated CO_2 conditions, an increase of 22% in assimilation rate was observed in the ILs in comparison to M82 plants (Figure 6A). In addition, C_i was significantly increased in all genotypes, without significant differences among genotypes (Figure 6C). ETR was again increased in the IL 2-5 and IL 2-6, 31 and 21% respectively in comparison with M82 plants (Figure 6D). Photorespiration (P_r) was significantly increased in ILs (Figure 6E), whereas no changes between ILs and M82 plants were observed for g_s and R_d at high CO_2 (Figure 6B and 6F).

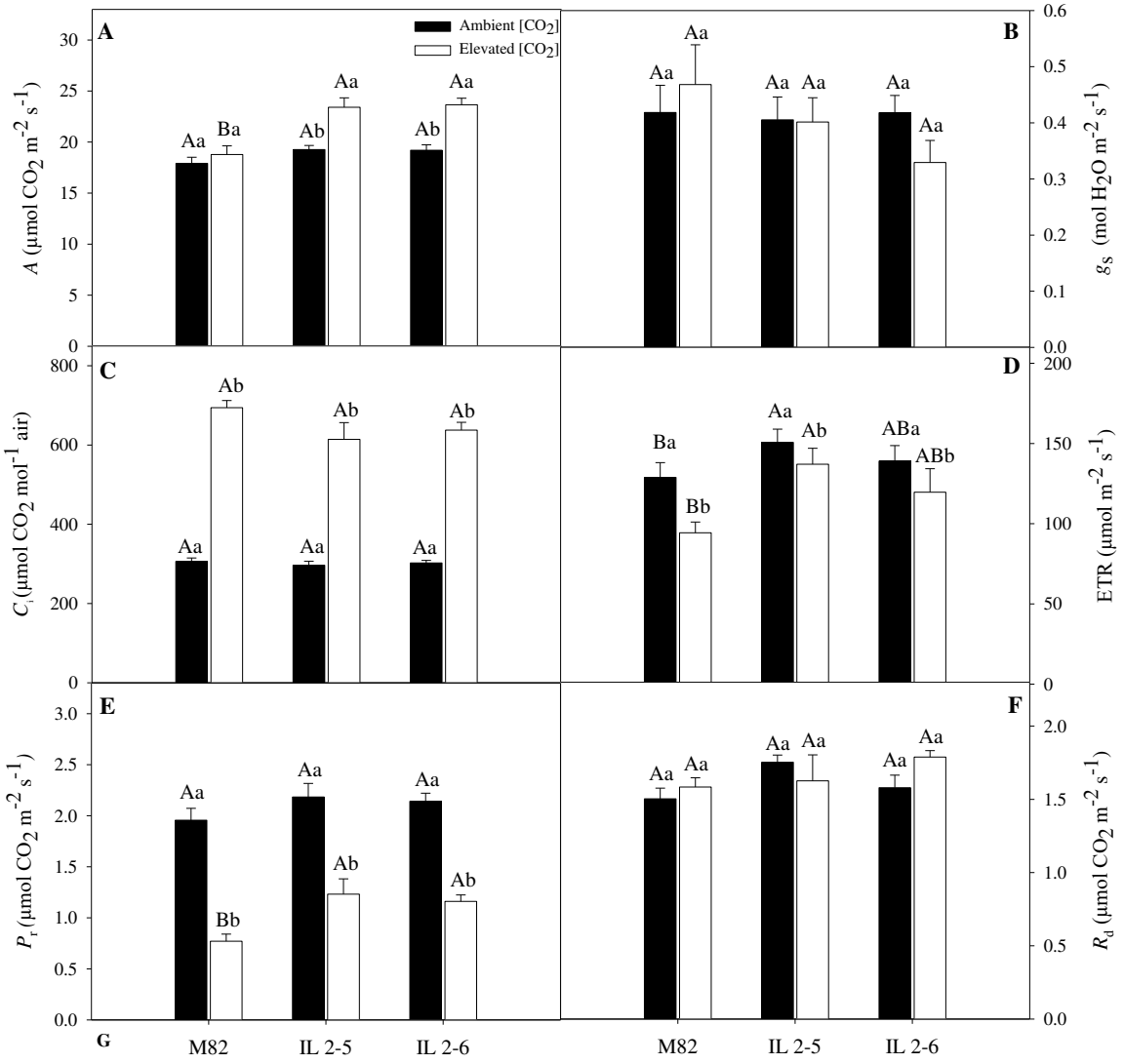

Figure 6. Gas exchange and fluorescence parameters of 4-week-old plants from two ILs of *Solanum pennellii* into a genetic background of *Solanum lycopersicum* (M82) grown at 400 or 800 µmol CO_2 mol^{-1}.

Assimilation rate **(A)**; Stomatal conductance **(B)**; Substomatal CO_2 concentration **(C)**; Electron transport rate **(D)**; Photorespiration **(E)**; Dark respiration **(F)**. Values are presented as means ± *SE* (n = 4). Means followed by different capital letters indicate significant differences among the genotypes, Tukey, $P < 0.05$. Different lowercase letters indicate significant differences among treatments Tukey, $P < 0.05$.

To obtain further information concerning the alteration in primary metabolism in the ILs at elevated CO_2 concentration, we next analyzed the levels of the major leaf metabolites (Figure 7). In agreement with previous results suggesting higher photosynthetic efficiency of both ILs under elevated CO_2 concentration, significant increase in the total chlorophyll and protein contents at the middle of the day, as well as fructose at the end of the dark period was verified for ILs (Figure 7A, 7D and 7F). Whilst sucrose at the end of the dark period increased in IL 2-5, it reduced in IL 2-6 in ambient and elevate CO_2 compared to M82 (Figure 7G). On the other hand, leaf chlorophyll *a*/*b* ratio, total amino acids, as well as glucose, fructose and sucrose contents were unaltered at the middle of the light period in both ambients (Figure 7B, 7C, 7E, 7F and 7G). Similar to the previous observations under ambient CO_2, an increase in starch levels was observed in plants from both ILs in comparison with plants from M82 cultivar at the middle of the light period (Figure 7H). Noteworthy, there was an increase in starch levels at the middle of the light period in all genotypes under elevate CO_2, nevertheless the ILs exhibited higher starch levels in relation to M82 (Figure 7H).

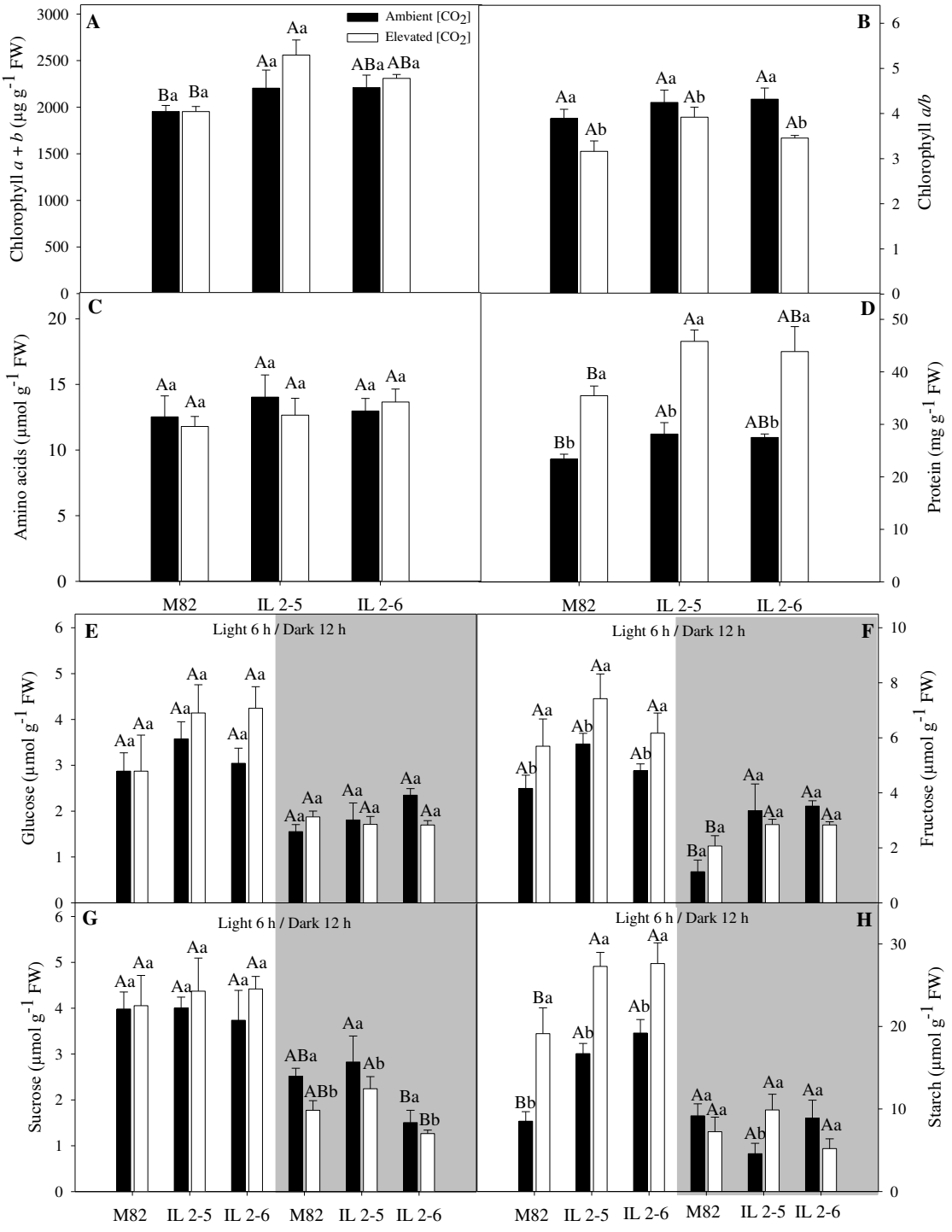

Figure 7. Metabolite levels of 4-week-old plants from two ILs of *Solanum pennellii* into a genetic background of *Solanum lycopersicum* (M82) grown at 400 or 800 µmol CO_2 mol^{-1}. Metabolite levels were measured in leaves at the middle of the light period (white sectors) and the end of dark period (gray sectors).

Chlorophyll *a* + *b* **(A);** Chlorophyll *a/b* ratio **(B);** Amino acids **(C);** Protein **(D);** Glucose **(E);** Fructose **(F);** Sucrose **(G);** Starch **(H)**. Values are presented as means ± *SE* (n = 4). Means followed by different capital letters indicate significant differences among the genotypes, Tukey, $P < 0.05$. Different lowercase letters indicate significant differences among treatments Tukey, $P < 0.05$.

5. DISCUSSION

The results obtained here demonstrated that the ILs have enhanced photosynthetic efficiency in comparison to the M82 cultivar, especially under elevated CO_2 concentration. In addition, it was demonstrated that the increase in photosynthetic efficiency is not related to diffusive properties, since g_s and g_m did not differ between the genotypes. Indeed, a large scale analysis of published data for 54 species demonstrated that the relationship between photosynthesis and internal conductance is actually not linear (Warren & Adams, 2006). Connecting physiological and biochemical approaches, we supply additional evidence that photosynthetic efficiency observed in the ILs is probably influenced by alteration in photochemical and biochemical reactions playing a role in growth modulation associated with carbon and nitrogen metabolisms. In agreement, photochemical reactions positively influence photosynthesis in other ILs (de Oliveira Silva et al., 2018).

Analyzing photosynthetic light-response data, a substantial increasing in $1/\phi$, which is a measure of photosynthetic efficiency (Tazoe et al., 2008), was noted in the ILs (Supplementary table 1). The variance in $1/\phi$ corroborates in part with the enhanced J_{flu} values in the ILs that might be allowing higher ATP and NADPH production for CO_2 fixation (Table 1). We should also report that high $1/\phi$ values reflect the non-photoinhibition of photosynthetic apparatus (Singsaas et al., 2001). Otherwise, evaluating the biochemical limitations data, high values of V_{cmax} and J_{max} also suggest higher capacity for CO_2 fixation in the ILs (Table 2). These parameters are related in such way that they contribute to equilibrium in the nitrogen allocation among proteins of the photosynthetic apparatus in order to maintain an adequate balance between carboxylation and RuBP regeneration rates (Walker et al., 2014). In addition, a negative correlation between C_c and $V_{cmax}\_C_c$ was identified (Table 2). Increase in CO_2 assimilation rates without changes in g_s result in decreased C_c (Fanourakis et al., 2015). In addition, even with higher SLA in the IL 2-5, changes in g_m were not noted.

A positive correlation has been proposed between starch and total protein content, which together have been show to contribute to the regulation of biomass production (Sulpice et al., 2009). At the same time that the ILs displayed biomass accumulation reflected in the leaf area (Figure 1A), which is a key determinant of carbon gain (Smith & Stitt, 2007; Irving, 2015), both ILs also exhibited higher leaf protein content (Figure 4C) that in turn is directly related to substantial levels of Rubisco. This assumption was

supported by Western blot analysis (Figure 5) in which RbcL proteins are relatively more abundant in the leaves of ILs than M82, supporting high values of the V_{cmax} (Hikosaka, 2004). Western blot analysis corroborated with greater photochemical efficiency satisfying the demands of higher foliar growth. Despite of that, only minor changes in initial or total Rubisco *in vitro* activity were verified in ILs (Supplementary figure 3). When we look at the higher level of carbohydrate in the ILs, the unchanged Rubisco activity values are possibly due to an adjustment of photosynthetic machinery in response to accumulation of starch (Caspar et al., 1985; Paul & Foyer, 2001).

The ILs which exhibited higher photosynthetic capacity also display higher fruit number (Semel et al., 2006) and enhanced accumulation of carboxylic acid (malate and citrate) levels by up 50% in fruits (only IL 2-5; Morgan et al., 2013). Apparently, such results indicate that the increase in photosynthetic capacity might influence on fruit composition and productivity of these lines.

We have clearly verified that CO_2 enrichment results in a substantial increase in the photosynthesis (~22%) and electron transport rate (~30%) in both ILs (Figure 6A and 6D). Despite higher CO_2 fixation in the ILs as indicated by elevated ETR values, which is expected to alter in elevated CO_2 (Naumburg & Ellsworth, 2000; Ghannoum et al., 2010; Li et al., 2013), g_s did not change in the ILs under high CO_2 concentration (Figure 6B). Given the unchanged g_s as well as the decrease in E in the ILs, these displayed higher WUE and WUE_i under normal and elevate CO_2 conditions (Supplementary figure 6B and 6C). These results corroborate with the higher $\delta^{13}C$ values found for the IL 2-5 suggesting an increased photosynthetic capacity over time and also a greater survival in an environment with low water availability (Xu et al., 2008). It seems reasonable to suggest that the ILs were not able to acclimatize to elevated CO_2 extended by short period. Probably, the highest C_i associated with the higher photosynthetic efficiency of the ILs resulted in an enhanced A at elevated CO_2.

The higher photosynthetic rate in plants under elevated CO_2 is due in part to the reduction in P_r, since Rubisco oxigenase side reaction is avoided by high CO_2 concentration (von Caemmerer & Farquhar, 1981; Stitt et al., 1991). Our findings are apparently in agreement with the widely assumption that P_r is suppressed at high CO_2 concentrations (Figure 6E). Nevertheless, both ILs exhibited higher values of estimated P_r under high CO_2 (Figure 6E). Based on the fact that the higher chlorophyll content and ETR rates may be leading to the increased production of ATP and NADPH in the ILs at elevated CO_2, probably P_r acts protecting the photosynthetic metabolism of

photoinhibition (Takahashi et al., 2007; Bauwe et al., 2012). This hypothesis is supported by previous studies showing that mutant plants with perturbation in the photorespiratory pathway display reduced *A*, rapidly photoinhibition and exhibit the repair system of the PSII D1 protein less effective (Timm et al., 2012). In addition, the impaired photosynthetic capacity in the same mutants was also reflected by reduced electron transport rate and enhanced non-photochemical quenching (Eisenhut et al., 2017). In a recent study, *A* as well as components of photosynthetic capacity, V_{cmax} and J_{max}, were also correlated with phenotypic variation in photorespiratory process (Tomeo & Rosenthal, 2018).

Among the metabolites measured in plants under elevated CO_2, chlorophyll, protein and starch showed a higher accumulation in ILs (Figure 7A, 7D, 7H). Close association between carbon and nitrogen metabolisms have been demonstrated in plants (Foyer et al., 1998; Araújo et al., 2008; Gauthier et al., 2010). Thus any alteration in carbon abundance is expected to reflect in nitrogen levels (Gutschick, 1999; Lambers et al., 2008; Nunes-Nesi et al., 2010). Higher chlorophyll content can be explained as a form to enhance the carbon assimilation of plants submitted to high CO_2 (Bhatt et al., 2010). The greatest photochemical efficiency and higher carbon assimilation were a determining factor for the increased starch content, without however retroinhibiting the photosynthetic process. In agreement with that, the sugar levels did not accumulate in both ILs, reflecting the capacity in which it was carried out to sink organs (Figure 7E-G). Thereafter, the high protein levels of ILs could mean a higher demand for proteins involved in the metabolism and export of carbohydrates resulting from the higher photosynthetic rate. Taken together, these results strongly indicated that carbon and nitrogen metabolism were altered in both ILs under ambient and high CO_2 conditions and are related with their higher photosynthetic efficiencies.

6. CONCLUSION

In summary, our study provides a step forward in understanding of physiological factors involved in the up regulation of photosynthetic capacity on chromosome 2 of ILs 2-5 and 2-6. Our findings indicated that the genetic variation on photosynthetic capacity in plants under normal and high CO_2 condition was mainly caused by variation in electron transport, V_{cmax}, J_{max} and Rubisco level with positive alterations in growth, as well as carbon and nitrogen metabolisms, suggesting that the products of the electron transport

rate were effectively translated into incorporation of biomass. Although IL 2-5 and IL 2-6 share the same QTL and exhibit common characteristics, phenotypic variation still exist between these lines. While the IL 2-5 displayed higher number of leaves and specific leaf area, the IL 2-6 exhibited a higher total dry weight. Remarkable, the higher photosynthetic capacity in IL 2-5 occurred associated with a higher carbon isotope composition and water use efficiency. Thus, the introgression sublines with introgressed fragments smaller than the original set of ILs (Alseekh et al., 2013) are an alternative to reduce genetic variance and the amount of gene to be analyzed; consequently, shortening the detection of the genes influencing photosynthetic capacity in tomato crops.

7. REFERENCES

Alseekh S., Ofner I., Pleban T., Tripodi P., Di Dato F., Cammareri M., … Zamir D. (2013) Resolution by recombination: Breaking up *Solanum pennellii* introgressions. *Trends in Plant Science* **18**, 536–538.

Araújo W.L., Nunes-Nesi A., Trenkamp S., Bunik V.I. & Fernie A.R. (2008) Inhibition of 2-oxoglutarate dehydrogenase in potato tuber suggests the enzyme is limiting for respiration and confirms its importance in nitrogen assimilation. *Plant physiology* **148**, 1782–96.

Bauwe H., Hagemann M., Kern R. & Timm S. (2012) Photorespiration has a dual origin and manifold links to central metabolism. *Current Opinion in Plant Biology* **15**, 269–275.

Baxter C.J., Carrari F., Bauke A., Overy S., Hill S.A., Quick P.W., … Sweetlove L.J. (2005) Fruit carbohydrate metabolism in an introgression line of tomato with increased fruit soluble solids. *Plant and Cell Physiology* **46**, 425–437.

Bhatt R.K., Baig M.J., Tiwari H.S. & Roy S. (2010) Growth, yield and photosynthesis of Panicum maximum and Stylosanthes hamata under elevated CO2. *Journal of environmental biology* **31**, 549–52.

Bolger A., Scossa F., Bolger M.E., Lanz C., Maumus F., Tohge T., … Fernie A.R. (2014) The genome of the stress-tolerant wild tomato species Solanum pennellii. *Nature Genetics* **46**, 1034–1038.

Bradford M.M. (1976) A rapid and sensitive method for the quantitation of microgram quantities of protein utilizing the principle of protein-dye binding. *Analytical Biochemistry* **72**, 248–254.

Bremner J.M. & Mulvaney C.S. (1965) Total Nitrogen. In *Methods of Soil Analysis*. pp. 595–622.

Caemmerer S. von (2000) *Biochemical models of leaf photosynthesis.* CSIRO Publishing.

von Caemmerer S. & Farquhar G.D. (1981) Some relationships between the biochemistry of photosynthesis and the gas exchange of leaves. *Planta* **153**, 376–387.

von Caemmerer S. & Farquhar G.D. (1984) Effects of partial defoliation, changes of irradiance during growth, short-term water stress and growth at enhanced p(C02)

on the photosynthetic capacity of leaves of Phaseolus vulgaris L. *Planta* **160**, 320–329.

Caspar T., Huber S.C. & Somerville C. (1985) Alterations in Growth, Photosynthesis, and Respiration in a Starchless Mutant of Arabidopsis thaliana (L.) Deficient in Chloroplast Phosphoglucomutase Activity. *Plant Physiology* **79**, 11–17.

Causse M., Duffe P., Gomez M.C., Buret M., Damidaux R., Zamir D., … Rothan C. (2004) A genetic map of candidate genes and QTLs involved in tomato fruit size and composition. *Journal of Experimental Botany* **55**, 1671–1685.

Charles H., Godfray H. & Garnett T. (2014) Food security and sustainable intensification. *Philosophical Transactions of the Royal Society B: Biological Sciences* **369**, 20120273.

Consortium T.T.G. (2012) The tomato genome sequence provides insights into fleshy fruit evolution. *Nature* **485**, 635–641.

Cross J.M., von Korff M., Altmann T., Bartzetko L., Sulpice R., Gibon Y., … Stitt M. (2006) Variation of enzyme activities and metabolite levels in 24 Arabidopsis accessions growing in carbon-limited conditions. *Plant physiology* **142**, 1574–88.

Cruz C.D. (2013) GENES - a software package for analysis in experimental statistics and quantitative genetics. *Acta Scientiarum* **35**, 271–276.

DaMatta F.M., Loos R.A., Silva E.A., Loureiro M.E. & Ducatti C. (2002) Effects of soil water deficit and nitrogen nutrition on water relations and photosynthesis of pot-grown Coffea canephora Pierre. *Trees - Structure and Function* **16**, 555–558.

Driever S.M., Lawson T., Andralojc P.J., Raines C.A. & Parry M.A.J. (2014) Natural variation in photosynthetic capacity, growth, and yield in 64 field-grown wheat genotypes. *Journal of Experimental Botany* **65**, 4959–4973.

Eisenhut M., Bräutigam A., Timm S., Florian A., Tohge T., Fernie A.R., … Weber A.P.M. (2017) Photorespiration Is Crucial for Dynamic Response of Photosynthetic Metabolism and Stomatal Movement to Altered CO2Availability. *Molecular Plant* **10**, 47–61.

Eshed Y. & Zamir D. (1995) An introgression line population of Lycopersicon pennellii in the cultivated tomato enables the identification and fine mapping of yield-associated QTL. *Genetics* **141**.

Ethier G.J. & Livingston N.J. (2004) On the need to incorporate sensitivity to CO2 transfer conductance into the Farquhar-von Caemmerer-Berry leaf photosynthesis model. *Plant, Cell and Environment* **27**, 137–153.

Fanourakis D., Giday H., Milla R., Pieruschka R., Kjaer K.H., Bolger M., … Ottosen C.-O. (2015) Pore size regulates operating stomatal conductance, while stomatal densities drive the partitioning of conductance between leaf sides. *Annals of Botany* **115**, 555–565.

Farquhar G.D., von Caemmerer S. & Berry J.A. (1980) A biochemical model of photosynthetic CO2 assimilation in leaves of C3 species. *Planta* **149**, 78–90.

Farquhar G.D., Ehleringer J.R. & Hubick K.T. (1989) Carbon Isotope Discrimination and Photosynthesis. *Annual Review of Plant Physiology and Plant Molecular Biology* **40**, 503–537.

Farquhar G.D. & Sharkey T.D. (1982) Stomatal Conductance and Photosynthesis. *Annual Review of Plant Physiology* **33**, 317–345.

Fernie A.R., Roscher A., Ratcliffe R.G. & Kruger N.J. (2001) Fructose 2,6-bisphosphate activates pyrophosphate: fructose-6-phosphate 1-phosphotransferase and increases triose phosphate to hexose phosphate cycling in heterotrophic cells. *Planta* **212**, 250–263.

Flexas J., Barbour M.M., Brendel O., Cabrera H.M., Carriquí M., Díaz-Espejo A., … Warren C.R. (2012) Mesophyll diffusion conductance to CO2: An unappreciated central player in photosynthesis. *Plant Science* **193**–**194**, 70–84.

Flexas J., Diaz-Espejo A., Galmés J., Kaldenhoff R., Medrano H. & Ribas-Carbo M. (2007) Rapid variations of mesophyll conductance in response to changes in CO 2 concentration around leaves. *Plant, Cell and Environment* **30**, 1284–1298.

Flood P.J., Harbinson J. & Aarts M.G.M. (2011) Natural genetic variation in plant photosynthesis. *Trends in Plant Science* **16**, 327–335.

Foyer C.H., Valadier M.-H., Migge A. & Becker T.W. (1998) Drought-induced effects on nitrate reductase activity and mRNA and on the coordination of nitrogen and carbon metabolism in maize leaves. *Plant physiology* **117**, 283–92.

Frary A., Göl D., Keleş D., Ökmen B., Pınar H., Şığva H.Ö., … Doğanlar S. (2010) Salt tolerance in Solanum pennellii: antioxidant response and related QTL. *BMC Plant Biology* **10**, 58.

Galmés J., Conesa M.A., Ochogavía J.M., Perdomo J.A., Francis D.M., Ribas-Carbó M., … Cifre J. (2011) Physiological and morphological adaptations in relation to water use efficiency in Mediterranean accessions of Solanum lycopersicum. *Plant, Cell and Environment* **34**, 245–260.

Galmés J., Kapralov M. V., Andralojc P.J., Conesa M.À., Keys A.J., Parry M.A.J. &

Flexas J. (2014) Expanding knowledge of the Rubisco kinetics variability in plant species: environmental and evolutionary trends. *Plant, Cell & Environment* **37**, 1989–2001.

Gauthier P.P.G., Bligny R., Gout E., Mahé A., Nogués S., Hodges M. & Tcherkez G.G.B. (2010) In folio isotopic tracing demonstrates that nitrogen assimilation into glutamate is mostly independent from current CO2 assimilation in illuminated leaves of Brassica napus. *New Phytologist* **185**, 988–999.

Geber M.A. & Dawson T.E. (1997) Genetic variation in stomatal and biochemical limitations to photosynthesis in the annual plant, Polygonum arenastrum. *Oecologia* **109**, 535–546.

Genty B., Briantais J.-M. & Baker N.R. (1989) The relationship between the quantum yield of photosynthetic electron transport and quenching of chlorophyll fluorescence. *Biochimica et Biophysica Acta (BBA) - General Subjects* **990**, 87–92.

Ghannoum O., Phillips N.G., Sears M.A., Logan B.A., Lewis J.D., Conroy J.P. & Tissue D.T. (2010) Photosynthetic responses of two eucalypts to industrial-age changes in atmospheric [CO2] and temperature. *Plant, Cell & Environment* **33**, 1671–1681.

Gibon Y., Blaesing O.E., Hannemann J., Carillo P., Höhne M., Hendriks J.H.M., … Stitt M. (2004) A Robot-Based Platform to Measure Multiple Enzyme Activities in Arabidopsis Using a Set of Cycling Assays: Comparison of Changes of Enzyme Activities and Transcript Levels during Diurnal Cycles and in Prolonged Darkness. *The Plant Cell* **16**, 3304–3325.

Gong P., Zhang J., Li H., Yang C., Zhang C., Zhang X., … Ye Z. (2010) Transcriptional profiles of drought-responsive genes in modulating transcription signal transduction, and biochemical pathways in tomato. *Journal of Experimental Botany* **61**, 3563–3575.

Gonzalez-Martinez S.C., Krutovsky K. V & Neale D.B. (2006) Forest-tree population genomics and adaptive evolution doi:10.1111/j.1469-8137.2006.01686.x. *New Phytologist* **170**, 227–238.

Grassi G. & Magnani F. (2005) Stomatal, mesophyll conductance and biochemical limitations to photosynthesis as affected by drought and leaf ontogeny in ash and oak trees. *Plant, Cell and Environment* **28**, 834–849.

Gutschick V.P. (1999) Research reviews Biotic and abiotic consequences of differences in leaf structure. *New Phytologist* **143**, 3–18.

Harley P.C., Loreto F., Marco G. Di & Sharkey T.D. (1992) Theoretical Considerations when Estimating the Mesophyll Conductance to CO2 Flux by Analysis of the Response of Photosynthesis to CO2. *Plant Physiology* **98**, 1429.

Hermida-Carrera C., Kapralov M. V & Galmés J. (2016) Rubisco Catalytic Properties and Temperature Response in Crops 1. *Plant Physiology* **171**, 2549–2561.

Hikosaka K. (2004) Interspecific difference in the photosynthesis - nitrogen relationship: patterns, physiological causes, and ecological importance. *Journal of Plant Research* **117**, 481–494.

Hunt R., Causton D.R., Shipley B. & Askew A.P. (2002) A modern tool for classical plant growth analysis. *Annals of botany* **90**, 485–8.

Irving L. (2015) Carbon Assimilation, Biomass Partitioning and Productivity in Grasses. *Agriculture* **5**, 1116–1134.

Ishii H., Hamada Y. & Utsugi H. (2012) Variation in light-intercepting area and photosynthetic rate of sun and shade shoots of two Picea species in relation to the angle of incoming light. *Tree Physiology* **32**, 1227–1236.

Lambers H., Chapin F.S. & Pons T.L. (2008) Photosynthesis. In *Plant Physiological Ecology*. pp. 11–99. Springer New York, New York, NY.

Leakey A.D.B., Ainsworth E.A., Bernacchi C.J., Rogers A., Long S.P. & Ort D.R. (2009) Elevated CO 2 effects on plant carbon, nitrogen, and water relations: six important lessons from FACE. *Journal of Experimental Botany* **60**, 2859–2876.

Lefebvre S., Lawson T., Fryer M., Zakhleniuk O. V, Lloyd J.C. & Raines C.A. (2005) Increased Sedoheptulose-1,7-Bisphosphatase Activity in Transgenic Tobacco Plants Stimulates Photosynthesis and Growth from an Early Stage in Development 1. *American Society of Plant Biologists 451 www.plantphysiol.org on November* **138**, 451–460.

Li X., Zhang G., Sun B., Zhang S., Zhang Y., Liao Y., … Yu J. (2013) Stimulated Leaf Dark Respiration in Tomato in an Elevated Carbon Dioxide Atmosphere. *Scientific Reports* **3**, 3433.

Liu Y.-S., Gur A., Ronen G., Causse M., Damidaux R., Buret M., … Zamir D. (2003) There is more to tomato fruit colour than candidate carotenoid genes. *Plant Biotechnology Journal* **1**, 195–207.

Logan, B.A. Adams, W.W. III Demmig-Adams B. (2007) Avoiding common pitfalls of chlorophyll fluorescence analysis under field conditions. *Functional plant biology* **34**, 853–859.

Mathan J., Bhattacharya J. & Ranjan A. (2016) Enhancing crop yield by optimizing plant developmental features. *Development* **143**, 3283–3294.

Miyagawa Y., Tamoi M. & Shigeoka S. (2001) Overexpression of a cyanobacterial. *Nature biotechnology* **19**, 965–969.

Morgan M.J., Osorio S., Gehl B., Baxter C.J., Kruger N.J., Ratcliffe R.G., … Sweetlove L.J. (2013) Metabolic Engineering of Tomato Fruit Organic Acid Content Guided by Biochemical Analysis of an Introgression Line. *Plant Physiology* **161**, 397–407.

Muir C.D., Pease J.B. & Moyle L.C. (2014) Quantitative genetic analysis indicates natural selection on leaf phenotypes across wild tomato species (Solanum sect. lycopersicon; solanaceae). *Genetics* **198**, 1629–1643.

Naumburg E. & Ellsworth D.S. (2000) Photosynthetic sunfleck utilization potential of understory saplings growing under elevated CO2 in FACE. *Oecologia* **122**, 163–174.

Nunes-nesi A., Carrari F., Gibon Y., Sulpice R., Lytovchenko A., Fisahn J., … Fernie A.R. (2007) Deficiency of mitochondrial fumarase activity in tomato plants impairs photosynthesis via an effect on stomatal function. *The Plant Journal* **50**, 1093–1106.

Nunes-Nesi A., Fernie A.R. & Stitt M. (2010) Metabolic and signaling aspects underpinning the regulation of plant carbon nitrogen interactions. *Molecular Plant* **3**, 973–996.

Nunes-Nesi A., Nascimento V.D.L., De Oliveira Silva F.M., Zsögön A., Araújo W.L. & Sulpice R. (2016) Natural genetic variation for morphological and molecular determinants of plant growth and yield. *Journal of Experimental Botany* **67**, 2989–3001.

de Oliveira Silva F.M., Lichtenstein G., Alseekh S., Rosado-Souza L., Conte M., Suguiyama V.F., … Nunes-Nesi A. (2018) The genetic architecture of photosynthesis and plant growth-related traits in tomato. *Plant Cell and Environment* **41**, 327–341.

Ort D.R., Merchant S.S., Alric J., Barkan A., Blankenship R.E., Bock R., … Ee Z. (2015) Redesigning photosynthesis to sustainably meet global food and bioenergy demand. *PNAS* **112**, 8529–8536.

Palmqvist K., Campbell D., Ekblad A. & Johansson H. (1998) Photosynthetic capacity in relation to nitrogen content and its partitioning in lichens with different photobionts. *Plant, Cell and Environment* **21**, 361–372.

Paul M.J. & Foyer C.H. (2001) Sink regulation of photosynthesis\r10.1093/jexbot/52.360.1383. *Journal of Experimental Botany* **52**, 1383–1400.

Peterhansel C., Horst I., Niessen M., Blume C., Kebeish R., Kürkcüoglu S. & Kreuzaler F. (2010) Photorespiration. *The Arabidopsis Book* **8**, e0130.

Schneider C.A., Rasband W.S. & Eliceiri K.W. (2012) NIH Image to ImageJ: 25 years of image analysis. *Nature methods* **9**, 671–5.

Semel Y., Nissenbaum J., Menda N., Zinder M., Krieger U., Issman N., … Zamir D. (2006) Overdominant quantitative trait loci for yield and fitness in tomato. *Proceedings of the National Academy of Sciences* **103**, 12981–12986.

Sharkey T.D. Photosynthesis in Intact Leaves of C3 Plants: Physics, Physiology and Rate Limitations. *Botanical Review* **51**, 53–105.

Sharkey T.D., Bernacchi C.J., Farquhar G.D. & Singsaas E.L. (2007) Fitting photosynthetic carbon dioxide response curves for C 3 leaves. *Plant, Cell & Environment* **30**, 1035–1040.

Sharlach M., Dahlbeck D., Liu L., Chiu J., Jiménez-Gómez J.M., Kimura S., … Staskawicz B.J. (2013) Fine genetic mapping of RXopJ4, a bacterial spot disease resistance locus from Solanum pennellii LA716. *Theoretical and Applied Genetics* **126**, 601–609.

Singh J., Pandey P., James D., Chandrasekhar K., Achary V.M.M., Kaul T., … Reddy M.K. (2014) Enhancing C3 photosynthesis: An outlook on feasible interventions for crop improvement. *Plant Biotechnology Journal* **12**, 1217–1230.

Singsaas E.L., Ort D.R. & DeLucia E.H. (2001) Variation in measured values of photosynthetic quantum yield in ecophysiological studies. *Oecologia* **128**, 15–23.

Smith A.M. & Stitt M. (2007) Coordination of carbon supply and plant growth. *Plant, Cell & Environment* **30**, 1126–1149.

Steinhauser M.-C., Steinhauser D., Gibon Y., Bolger M., Arrivault S., Usadel B., … Stitt M. (2011) Identification of Enzyme Activity Quantitative Trait Loci in a Solanum lycopersicum x Solanum pennellii Introgression Line Population. *Plant physiology* **157**, 998–1014.

Stitt M., Quick W.P., Schurr U., Schulze E.-D., Rodermel S.R. & Bogorad L. (1991) Decreased ribulose-1,5-bisphosphate carboxylase-oxygenase in transgenic tobacco transformed with ?antisense? rbcS. *Planta* **183**, 555–566.

Sulpice R., Pyl E.-T., Ishihara H., Trenkamp S., Steinfath M., Witucka-Wall H., … Stitt

M. (2009) Starch as a major integrator in the regulation of plant growth. *Proceedings of the National Academy of Sciences* **106**, 10348–10353.

Sulpice R., Tschoep H., Von Korff M., BussisS D., Usadel B., Hohne M., … Gibon Y. (2007) Description and applications of a rapid and sensitive non-radioactive microplate-based assay for maximum and initial activity of D-ribulose-1,5-bisphosphate carboxylase/oxygenase. *Plant, Cell & Environment* **30**, 1163–1175.

Sundström J.F., Albihn A., Boqvist S., Ljungvall K., Marstorp H., Martiin C., … Magnusson U. (2014) Future threats to agricultural food production posed by environmental degradation, climate change, and animal and plant diseases – a risk analysis in three economic and climate settings. *Food Security* **6**, 201–215.

Takahashi S., Bauwe H. & Badger M. (2007) Impairment of the photorespiratory pathway accelerates photoinhibition of photosystem II by suppression of repair but not acceleration of damage processes in Arabidopsis. *Plant physiology* **144**, 487–94.

Tazoe Y., Hanba Y.T., Furumoto T., Noguchi K. & Terashima I. (2008) Relationships Between Quantum Yield for CO2 Assimilation, Activity of Key Enzymes and CO2 Leakiness in Amaranthus cruentus, a C4 Dicot, Grown in High or Low Light. *Plant and Cell Physiology* **49**, 19–29.

Tilman D., Cassman K.G., Matson P.A., Naylor R. & Polasky S. (2002) Agricultural sustainability and intensive production practices. *Nature* **418**, 671–677.

Timm S., Mielewczik M., Florian A., Frankenbach S., Dreissen A., Hocken N., … Bauwe H. (2012) High-to-low CO2acclimation reveals plasticity of the photorespiratory pathway and indicates regulatory links to cellular metabolism of Arabidopsis. *PLoS ONE* **7**.

Tomeo N.J. & Rosenthal D.M. (2018) Photorespiration differs among Arabidopsis thaliana ecotypes and is correlated with photosynthesis. *Journal of Experimental Botany* **69**, 5191–5204.

Tomimatsu H. & Tang Y. (2016) Effects of high CO2 levels on dynamic photosynthesis: carbon gain, mechanisms, and environmental interactions. *Journal of Plant Research* **129**, 365–377.

Towbin H., Staehelin T. & Gordon J. (1979) Electrophoretic transfer of proteins from polyacrylamide gels to nitrocellulose sheets: procedure and some applications. *Proceedings of the National Academy of Sciences of the United States of America* **76**, 4350–4.

Valentini R., Epron D., de Angelis P., Matteucci G. & Dreyer E. (1995) In situ estimation of net CO2assimilation, photosynthetic electron flow and photorespiration in Turkey oak (Q. cerris L.) leaves: diurnal cycles under different levels of water supply. *Plant, Cell & Environment* **18**, 631–640.

Vasconcelos É.A.R., Nogueira F.C.S., Abreu E.F.M., Gonçalves E.F., Souza P.A.S. & Campos F.A.P. (2005) Protein Extraction From Cowpea Tissues for 2-D Gel Electrophoresis and MS Analysis. *Chromatographia* **62**, 447–450.

Vrá Bl D., Vaš Ková M., Hronková M., Flexas J. & ˇ Antrů C ˇ Ek J.S. (2009) Mesophyll conductance to CO 2 transport estimated by two independent methods: effect of variable CO 2 concentration and abscisic acid. *Journal of Experimental Botany* **60**, 2315–2323.

Walker A.P., Beckerman A.P., Gu L., Kattge J., Cernusak L.A., Domingues T.F., … Woodward F.I. (2014) The relationship of leaf photosynthetic traits - V_{cmax} and J_{max} - to leaf nitrogen, leaf phosphorus, and specific leaf area: a meta-analysis and modeling study. *Ecology and Evolution* **4**, 3218–3235.

Warren C.R. & Adams M.A. (2006) Internal conductance does not scale with photosynthetic capacity: Implications for carbon isotope discrimination and the economics of water and nitrogen use in photosynthesis. *Plant, Cell and Environment* **29**, 192–201.

Weraduwage S.M., Chen J., Anozie F.C., Morales A., Weise S.E. & Sharkey T.D. (2015) The relationship between leaf area growth and biomass accumulation in Arabidopsis thaliana. *Frontiers in Plant Science* **6**, 1–21.

Woodrow I.E. & Berry J.A. (1988) Enzymatic Regulation of Photosynthetic CO2, Fixation in C3 Plants. *Annual Review of Plant Physiology and Plant Molecular Biology* **39**, 533–594.

Xu X., Martin B., Comstock J.P., Vision T.J., Tauer C.G., Zhao B., … Knapp S. (2008) Fine mapping a QTL for carbon isotope composition in tomato. *Theoretical and Applied Genetics* **117**, 221–233.

8. SUPPLEMENTARY DATA

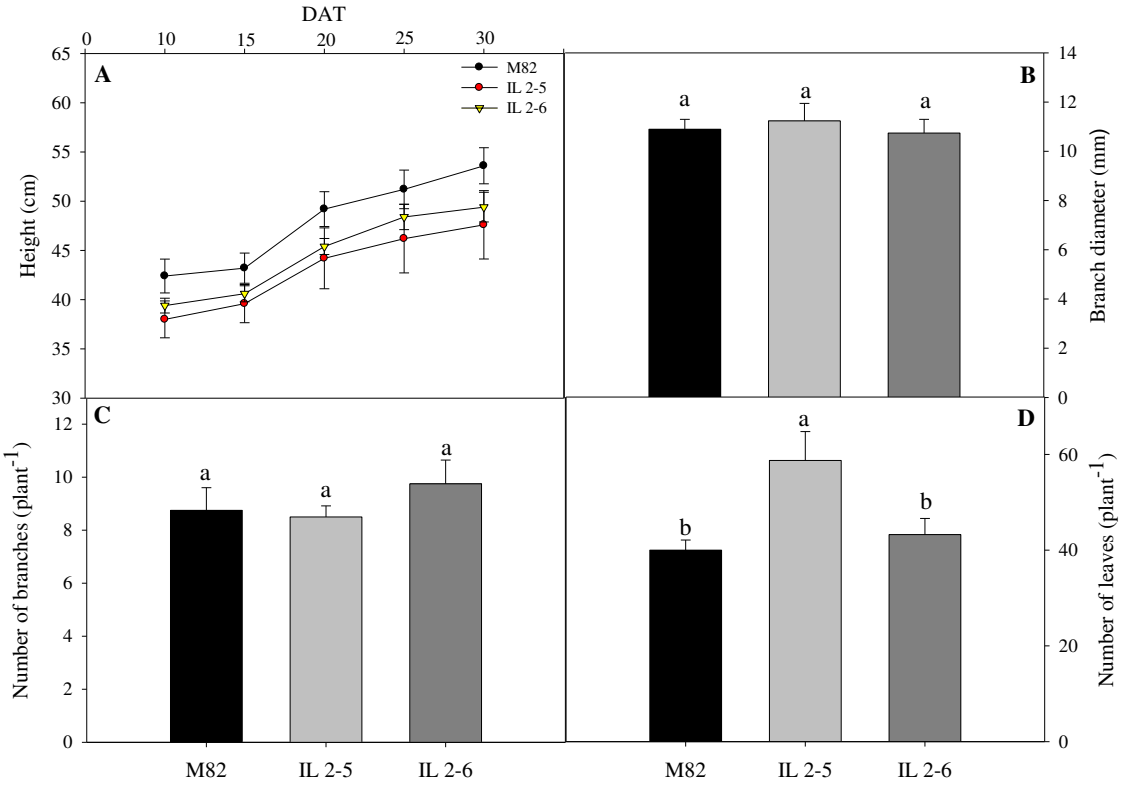

Supplementary figure 1. Growth phenotypes of 4-week-old plants from two ILs of *Solanum pennellii* into a genetic background of *Solanum lycopersicum* (M82). Height **(A)**; Branch diameter **(B)**; Number of branches **(C)**; Number of leaves **(D)**. Values are presented as means ± *SE* (n = 6). Means that differ significantly between ($P < 0.05$) by the Tukey test are accompanied by different letters. DAT: Days after transplanting.

Supplementary table 1. Photosynthetic parameters derived from light response curve of 4-week-old plants from two ILs of Solanum pennellii into a genetic background of Solanum lycopersicum (M82). Values are presented as means ± SE (n = 6). Means that differ significantly between ($P < 0.05$) by the Tukey test are accompanied by different letters.

Parameters*	**M82**	**IL 2-5**	**IL 2-6**
A_{max} (µmol CO_2 m^{-2} s^{-1})	22.39 ± 0.79 **a**	23.96 ± 0.72 **a**	23.54 ± 0.97 **a**
1/ϕ (mol/mol)	14.24 ± 0.43 **b**	16.42 ± 0.74 **a**	14.61 ± 0.50 **ab**
LCP (µmol m^{-2} s^{-1})	39.68 ± 1.64 **a**	45.60 ± 3.04 **a**	43.54 ± 2.92 **a**
LSP (µmol m^{-2} s^{-1})	699.52 ± 20.55 **a**	646.41 ± 29.57 **a**	731.40 ± 38.02 **a**

* A_{max}, maximum photosynthetic rate; 1/ϕ apparent quantum yield; LCP, light compensation point; LSP, light saturation point.

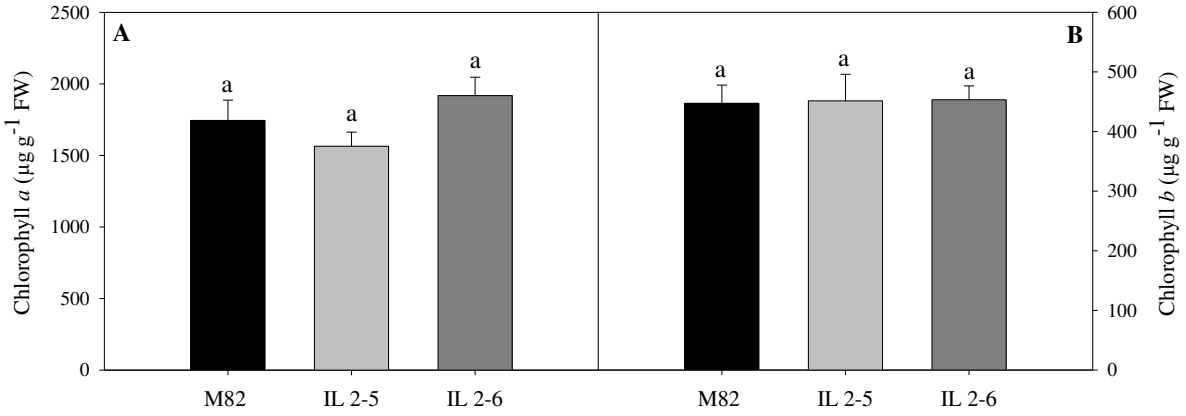

Supplementary figure 2. Chlorophyll content *a* and Chlorophyll content *b* of 4-week-old plants from two ILs of *Solanum pennellii* into a genetic background of *Solanum lycopersicum* (M82). Levels of chlorophyll *a* **(A);** Levels of chlorophyll *b* **(B).** Values are presented as means ± *SE* (n = 6). Means that differ significantly between ($P < 0.05$) by the Tukey test are accompanied by different letters. FW: Fresh weight.

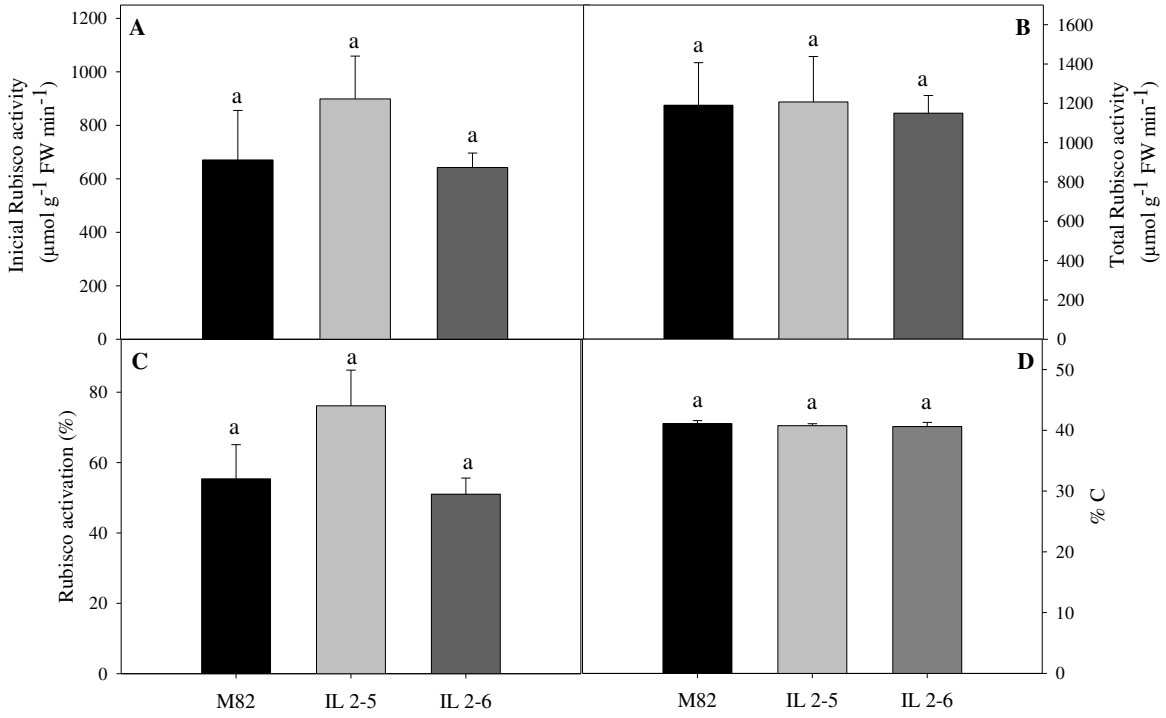

Supplementary figure 3. Rubisco activity and carbon percentage of 4-week-old plants from two ILs of *Solanum pennellii* into a genetic background of *Solanum lycopersicum* (M82). Initial Rubisco activity **(A);** Total Rubisco activity **(B);** Rubisco activation **(C)**; Carbon percentage **(D)**. Values are presented as means ± *SE* (n = 6). Means that differ significantly between ($P < 0.05$) by the Tukey test are accompanied by different letters. FW: Fresh weight.

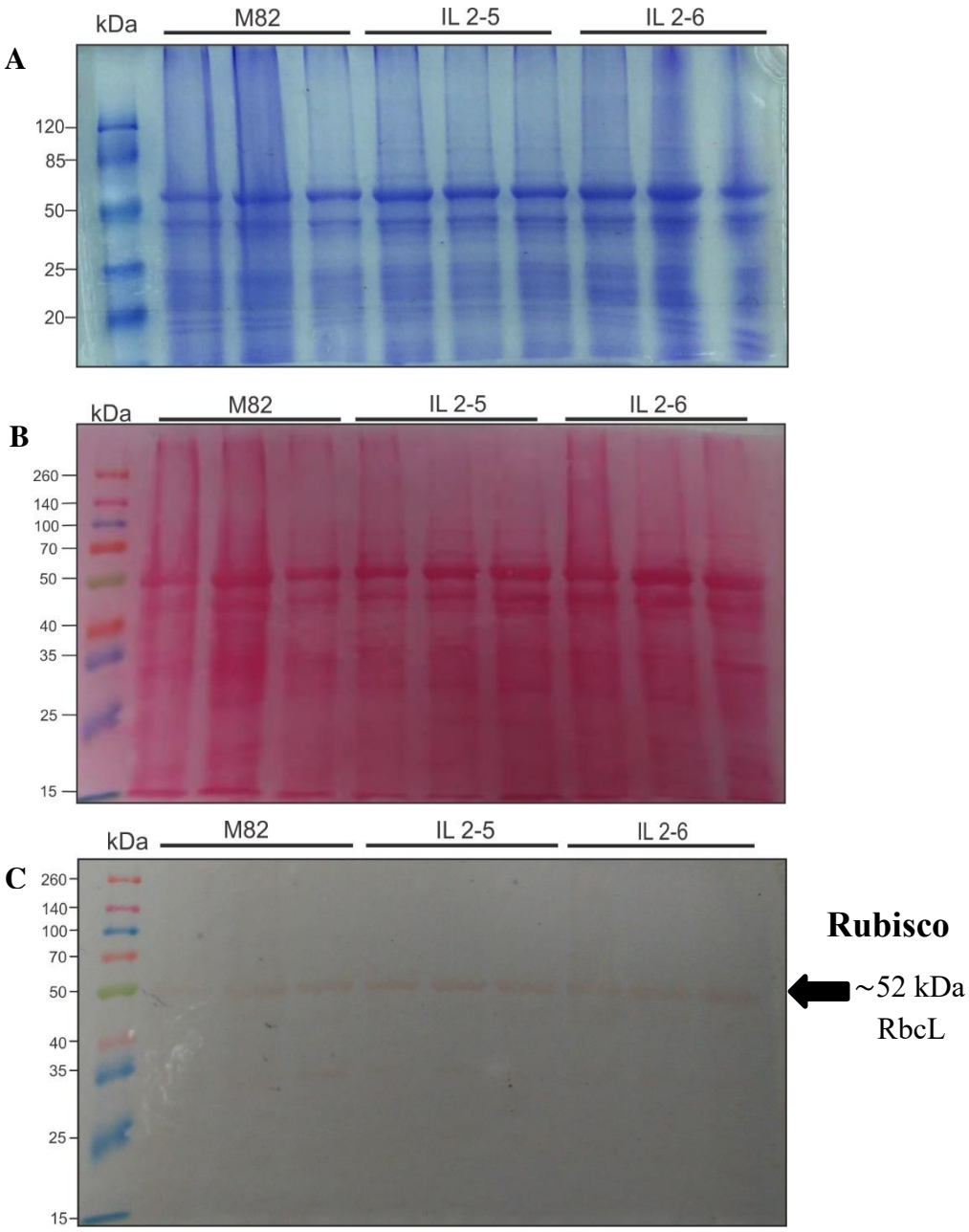

Supplementary figure 4. Levels of Rubisco large subunit (RbcL) in 4-week-old plants from two ILs of *Solanum pennellii* into a genetic background of *Solanum lycopersicum* (M82). Protein was loaded on a 12% SDS-PAGE and further stained with Coomassie brilliant blue (**A**); Nitrocellulose membrane stained with Ponceau **(B);** Nitrocellulose membrane revealed with 3,3′-diaminobenzidine (DAB) **(C).** RbcL designates the large subunit of ribulose-1,5-bisphosphate carboxylase/oxygenase.

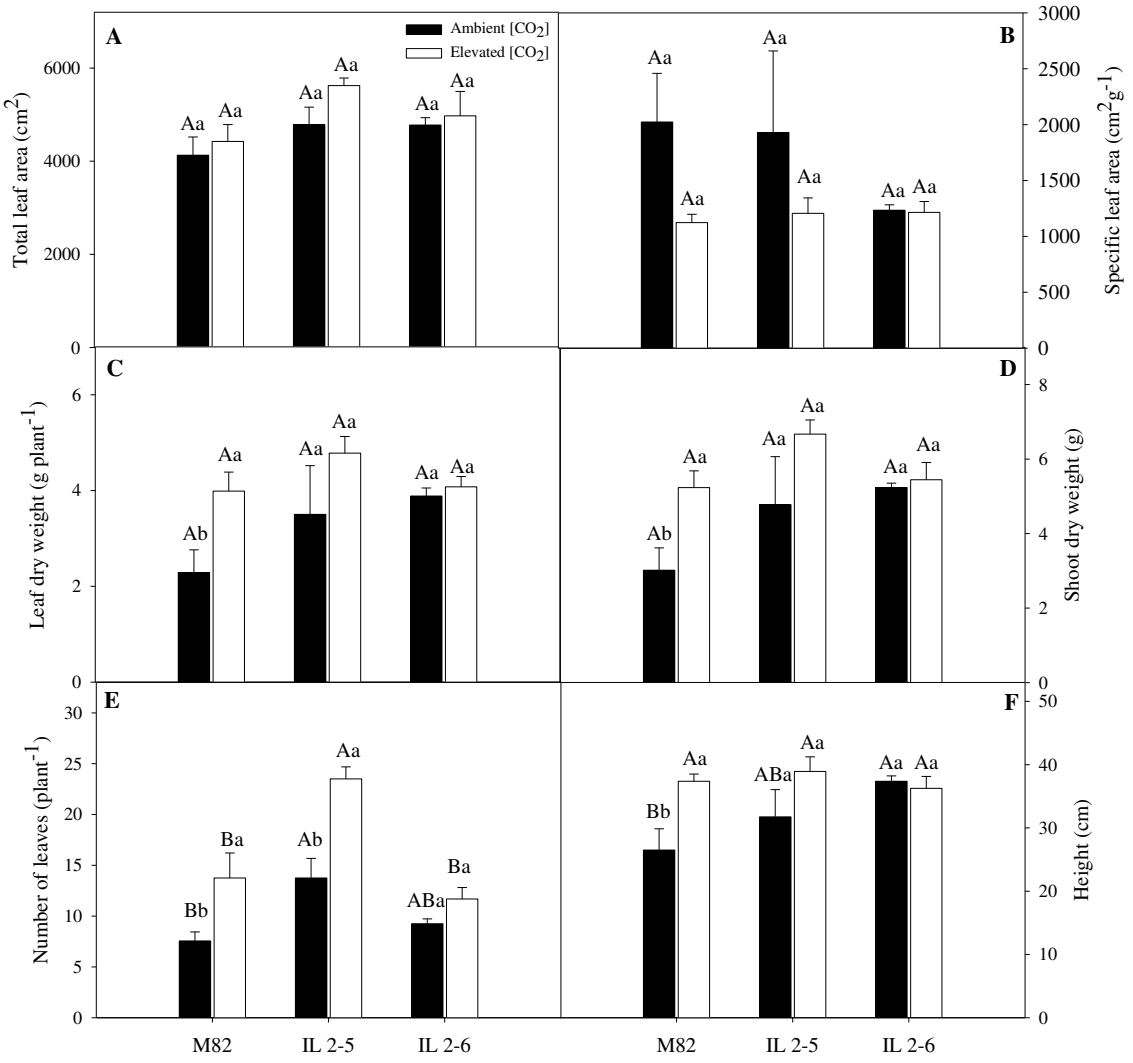

Supplementary figure 5. Growth phenotypes of 4-week-old plants from two ILs of *Solanum pennellii* into a genetic background of *Solanum lycopersicum* (M82) grown at 400 or 800 µmol CO_2 mol^{-1}.

Total leaf area **(A)**; Specific leaf area **(B);** Leaf dry weight **(C)**; Shoot dry weight **(D);** Number of leaves **(E);** Height **(F)**. Values are presented as means ± *SE* (n = 4). Means followed by different capital letters indicate significant differences among the genotypes, Tukey, $P < 0.05$. Different lowercase letters indicate significant differences among treatments Tukey, $P < 0.05$.

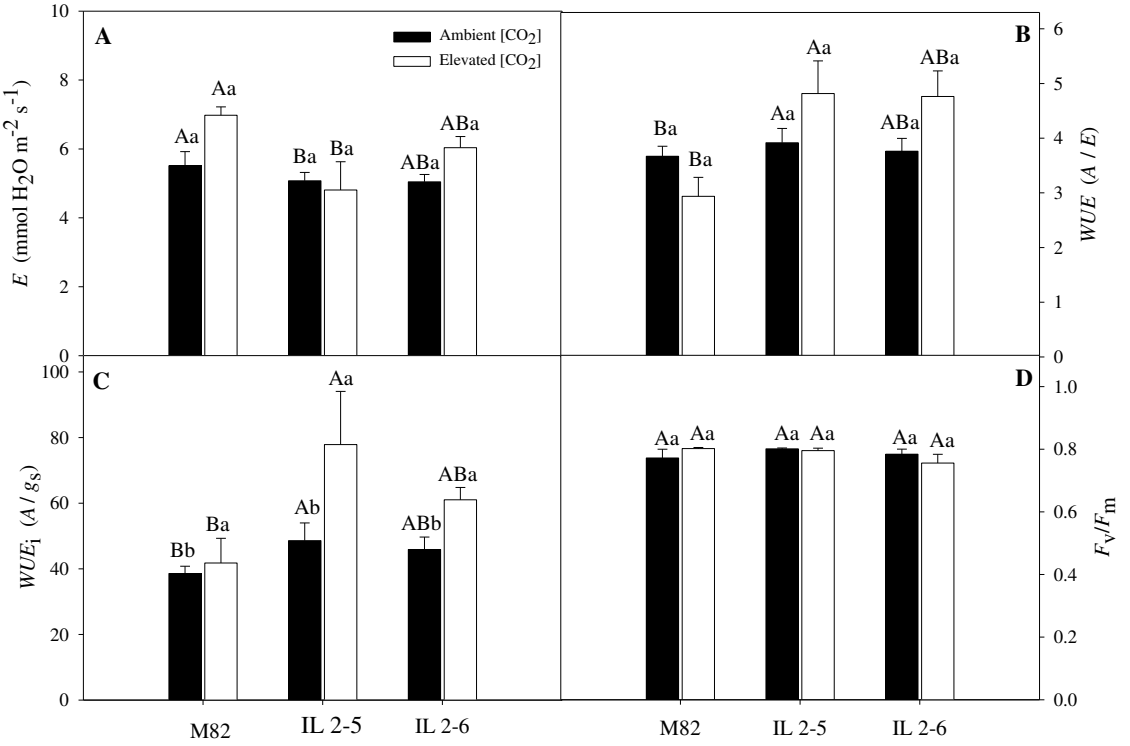

Supplementary figure 6. Gas exchange parameters of 30 days-old plants from two ILs of *Solanum pennellii* into a genetic background of *Solanum lycopersicum* (M82) grown at 400 or 800 µmol CO_2 mol^{-1}.

Transpiration **(A);** Water use efficiency **(B);** Intrinsic water use efficiency **(C)**; Maximum PSII photochemical efficiency **(D)**. Values are presented as means ± *SE* (n = 4). Means followed by different capital letters indicate significant differences among the genotypes, Tukey, $P < 0.05$. Different lowercase letters indicate significant differences among treatments Tukey, $P < 0.05$.

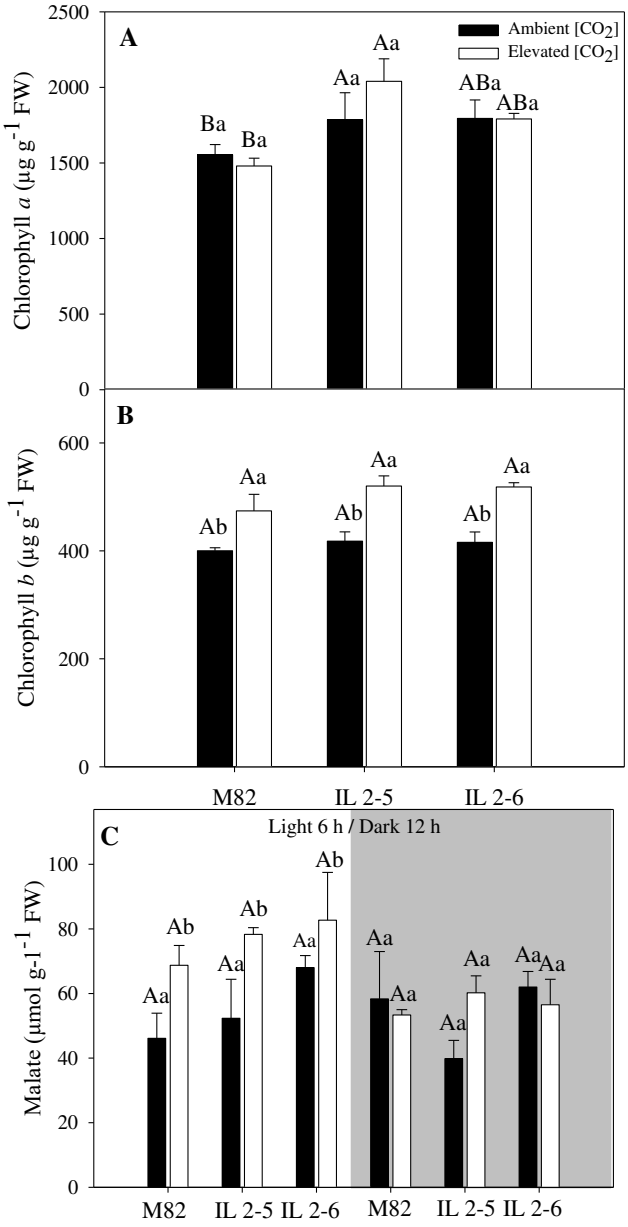

Supplementary figure 7. Chlorophyll (*a* + *b*) and malate content of 30 days-old plants from two ILs of *Solanum pennellii* into a genetic background of *Solanum lycopersicum* (M82) grown at 400 or 800 µmol CO_2 mol^{-1}.

Levels of chlorophyll *a* **(A);** Levels of chlorophyll *b* **(B);** Malate **(C)**. Values are presented as means ± *SE* (n = 4). Means followed by different capital letters indicate significant differences among the genotypes, Tukey, $P < 0.05$. Different lowercase letters indicate significant differences among treatments Tukey, $P < 0.05$.